Quasi 18-hour wave activity in ground-based observed mesospheric water vapor over Bern, Switzerland

Martin Lainer, Klemens Hocke, Rolf Rüfenacht, and Niklaus Kämpfer

---

Final Response on ACPD paper acp-2016-1050:

Color Code: Referee comments, Authors response, Link to relevant changes in manuscript

---

We would like to thank all anonymous referees for their efforts and comments which helped us to launch a revised manuscript version. This new version only focuses on the observations (mesospheric water vapor and wind) and the robustness of the analyzed data. The parts dealing with SD-WACCM model simulations and Aura MLS data are removed with regard to the reviewer comments. In consequence many comments will be answered only briefly due to the omission of manuscript parts.

Please find our point by point response to all three reviews below. A marked-up manuscript version is provided in the end.

1 Response to Referee #2

Major issues

(1)
WACCM model results: a resolution of 2.5° means that only waves with wavelength >400 km or so are resolved. So this is certainly a different part of the spectrum than observed with the microwave radiometer. Figs. 4 and 5 show that the spectra are completely different, and the only commonality is the height range, where the waves maximise. But this is only a similarity and one cannot really identify common waves in the model and observations.

We agree that the analysis of atmospheric wave parameters from the SD-WACCM model simulations and Aura MLS data was not sophisticated enough. As stated in the introduction, all parts in the manuscript dealing with WACCM or Aura MLS data are omitted now. This includes also the hodograph analysis, which was only performed with SD-WACCM data because the quality of the meridional wind observations by the Doppler wind radiometer WIRA was not good enough.

Section 2.3 is deleted. In Sect. 2 we now only describe the microwave radiometers and the corresponding data sets. In Sect. 4 the focus is put on the monthly mean H_2O

spectra (Sect. 4.1) and the temporal evolution of the 18-hour wave amplitudes in the H_2O and zonal wind data (Sect. 4.2). All parts and figures mentioning and showing SD-WACCM results are removed (Figs. 5, 7, 9, 10, 11c, 12). In Section 4, a new subsection 4.3 is included and discusses the obtained results in regard of inertia-gravity waves or the possibility of a non-linear wave-wave interaction between the quasi 2-day wave and the diurnal tide.

(2)
The hodograph analysis in Fig. 13 requires explanation. There is some theory given in section 3, but it is not well described what the authors really did to obtain the wave parameters. Obtaining the intrinsic frequency from ϵ (ratio between the major and minor axis of hodograph ellipse) and then using the Doppler relation to get the horizontal wavelength? How was the observed frequency defined, from the radiometer measurements? And what is the error of this analysis? If the intrinsic frequency and horizontal wavelength is known, the dispersion relation will give the vertical wavelength, but from Fig. 13 a vertical scale of some 20 km is visible, is it possible that the difference 20 km vs. <6 km comes from uncertainties of the analysis? ϵ is close to unity, and then a relatively small error might give a large relative error for the wavelength. WACCM cannot resolve waves with short vertical wavelength. The authors refer to Baumgarten et al. (2015), but in their wind and temperature residuals the short wavelength is immediately visible.

With our instruments alone we were not able to make use of the hodograph method. In principle it requires a higher vertical resolution than our microwave instruments can provide. Since the SD-WACCM part of the manuscript is deleted, it does not make sense any more to present the hodograph method and the simulated results.

Section 4.2.2 (Propagation analysis) is omitted together with Figs. 12 and 13. The manuscript part about the numerical methods is much shorter now and only explains the spectral data analysis we use.

(3)
Aura/EOS observations: The vertical resolution is less than 3 km, so I do not see how waves with wavelengths <6 km can be resolved. The description of Fig. 14 is not very clear. I assume that it shows temperature residual profiles every 12 hr? In the mesosphere, Fig. 14 shows maxima/minima constantly at the same level. This does not look like a real atmospheric phenomenon, and it rather seems as if these are the original data levels and the waves seen are due to aliasing. Analysis of Aura data therefore must be explained in much more detail, and possible effects of resolution have to be discussed. I doubt, however, that the results in Fig. 14 really show the gravity waves.

Our Aura MLS analysis is to a certain degree critical. If the vertical wavelength is less than 6 km the Nyquist sampling theorem is not valid for the vertical resolution of the MLS satellite data. However the result of a 6 km vertical wavelength is based on model data and might not describe the real atmospheric situation. But with our observations

we were not able to derive the vertical or horizontal wavelengths parameters. Based on the results of the SD-WACCM hodograph analysis, we agree that a MLS temperature profile analysis is more or less pointless.

Sections about Aura MLS and the temperature profiles (Sect. 2.2 and 4.3) is deleted, including Fig. 14.

Minor issues

(1)
P 2, introduction, l 13: The paragraph on the solar effects may be deleted. At least regarding the 11-year cycle, as the paper deals with gravity waves and not long-term, interannual variability.

We agree that the paragraph on the solar variability misses the point.

Therefore, the paragraph on solar variability is deleted in the introduction.

(2)
P3, L7: maybe replace frequency by angular frequency, at least when first introduced.

We agree, that it is more correct to use the term angular frequency.

In the discussion Section 4.3 we use the term angular frequency when first introduced.

(3)
P9, L20, Fig. 10: How was the correlation calculated? For each profile separately, so that the correlation is strong if the amplitudes maximise at the same height? This would not mean too much, in particular would not give information on whether the amplitudes appear simultaneously or not. If the correlation is insignificant, is it then simply set to zero?

It is correct that the correlation was calculated for each profile separately and set to zero if it was not significant (95 % confidence). However in the new manuscript version no comparison to SD-WACCM is performed any more.

Figure 10 is not presented any more in the results.

(4)
P11, L 13: temperature amplitudes, do you mean residuals or filtered temperatures as in Fig 14?

With temperature amplitudes we referred to as filtered temperatures. But no Aura MLS temperature data is shown in the revised version of the manuscript now.

Section 4.3 and Figure 14 is not part of the manuscript any more.

(5)
P11, L 21: how do you know that it is the 18 hr wave that is analysed from the temperature profiles?

It is correct that we cannot say that the high-pass filtered time series of the temperature profiles is only related to the 18 hour wave. Only the SD-WACCM hodograph analysis suggested that the inertia-gravity waves have vertical wavelengths below 6 km and that value was used as upper limit in the filter settings.

We do not show any MLS data now.

(6)
P 11, L 23: Which kind of temporal structures? Long-period variations of the waves?

Needless to answer, since MLS data is not shown any more.

Same as before. Section 4.3 is deleted.

(7)
Fig 13, caption: what means background wind speed?

The background wind speed is the projected true wind speed in the direction of wave propagation (obtained from the hodograph analysis). The background wind speed as shown in Figure 13 is not a 18-hour filtered component of u and v. Since the comparison between SD-WACCM and WIRA / MIAWARA data is questionable we do not apply the hodograph analysis in the new manuscript version.

Figure 13 and the presented results are omitted now.

2 Response to Referee #3

Major comment

Their result seems interesting, is broadly plausible and certainly suitable for ACP. My main question, and it's a serious one, is how can they actually observe this kind of oscillation in their H_2O data? Any wave in a conserved tracer field should only be manifest if the vertical gradient of the tracer is small enough relative to the vertical displace-

ment. The oscillations seen in their data (i.e. Figure 1) seem very large for what is supposedly only a 6 km vertical wavelength. And further, their vertical resolution seems insufficient to capture a 6 km wave. I am comfortable with a limb viewer such as MLS seeing this wave, but a vertical sounder seems less likely. On page 4, line 20, they give their vertical resolution as 11–14 km, but then say the 18 hour wave has 6 km vertical wavelength. If that is the case, then how can they see it? At a minimum, they need to present some simulations showing this. For example, the gravity wave community has spent considerable time and effort illustrating how waves are seen differently in limb vs. nadir sounders. Here, some sort of test case with an idealized wave is called for in order to be truly convincing, in my opinion. Or perhaps taking the WACCM fields and convolve them with the microwave averaging kernels. I'm worried that something else with a period of 18 hours is contaminating their retrieval and thus they are not actually seeing H_2O oscillations. The authors jump too quickly to spectral analysis without first presenting more raw data and showing how it varies. The same question applies to their wind data which has stated resolution of 10–16 km.

I guess with your statement "this kind of wave" you mean an inertia-gravity wave with a vertical wavelength below 6 km. You are right we would not be able to see such a wave. Have in mind that the 6 km wavelength was derived from the WACCM model. In consequence the 18-hour waves seen in WACCM and our water vapor or wind data are not comparable. From this point of view we even do not know if we see the effect of a inertia-gravity wave, which should then have a much larger vertical wavelength of at least ∼20 km. We decided to completely remove the WACCM data analysis and with it the propagation analysis of the hypothetical model resolved 18-hour inertia-gravity wave. The focus is now only on our ground-based observations. Unfortunately we have not the expertise on simulating inertia-gravity waves. Instead of our model based simulation to explain our wave observations we try to show that our retrievals are robust and not contaminated by possible 18-hour oscillations of instrument related parameters such as measurement response or various temperatures (outdoor, indoor, mixer, FPGA, Hot-Load, receiver).
We will also include more raw data. In case of MIAWARA water vapor we show monthly time series averaged between 0.02–0.1 hPa, which shows how the amount of H_2O varies in the altitude region where the 18-hour oscillation is observed. In case of the zonal wind measured by WIRA, we now show all observations which are available in December 2015. Since the whole SD-WACCM analysis is removed from the manuscript, a convolution by the microwave averaging kernels is redundant now.

We included new Figs. 2 and 3 showing monthly time series of MIAWARA H_2O averaged between 0.02–0.1 hPa. Fig. 4 shows now a longer zonal wind profile time series from the WIRA radiometer (2. Dec to 15 Dec.). Still the spectral analysis can only be performed between 5. Dec to 9. Dec., so the WIRA plot in Fig. 9 has not changed. In order to show that instrument related temperatures do not have a dominant 18-hour oscillation mode we exemplary show monthly mean wave spectra of 6 temperature time series for January, February and March 2016 (new Fig. 10). The results are presented

in the beginning of the new Section 4.3 (Discussion). The spectral analysis in the new Fig. 11 shows dominating oscillations in the a priori contribution (respectively measurement response) of the water vapor retrievals. We have not identified any prominent oscillations in the defined quasi 18-hour period band. Thus we conclude that we indeed observe real atmospheric wave oscillations in our data sets. Of course still it is not clear what causes these oscillations in the H_2O tracer field and zonal wind. Section 4.3 continuous to discuss about the inertia-gravity wave theory, but also on non-linear wave-wave interactions with regard to other published studies (eg. Li et al. (2007); Nicolls et al. (2010); Lieberman et al. (2017)

Minor comments

(1)
What is their integration time? On page 4, line 24, they say 3 hours. On page 5, line 22 they say 6.

On page 4, line 24 we were describing the MIAWARA water vapor retrieval and this uses an integration time of 3 hours. On the next page 5 line 22 we talk about the wind radiometer WIRA, which uses an integration time of 6 hours. Due to the omission of SD-WACCM and AURA MLS data, section 2 will now only present the ground-based microwave radiometers.

Old section 2 (Data sets) is renamed (Instruments and data sets) and splitted into two subsections: 2.1: Middle atmospheric water vapor radiometer and 2.2: Doppler wind radiometer. So the two used instruments are separately presented, which makes the structure more clear. Old subsections about SD-WACCM and Aura MLS are removed now.

(2)
If their measurement is only valid to 0.02 hPa (e.g. page 3), then they should cut off their plots at that level (e.g. Figures 1, 3, 6)

Yes, it is more convenient to cut off the H_2O related plots at the upper measurement limit of 0.02 hPa, except for Figure 1, where we show the MIAWARA H_2O time series together with the pressure level where the measurement response drops below 0.8.

As suggested from the referee, Figs. 3, 4, 6 and 8 are cut off at 0.02 hPa now.

(3)
End of abstract and beginning of Intro: They use “manifold” in adjacent sentences which seems awkward.

Thank you for the hint, we will replace the word manifold.

We changed the word “manifold” to “broad”.

(4)
Page 2, line 2: “Latter analyzed”...?

We suggest the following new expression:

We changed “Latter analyzed...” to “..., who analyzed ...”

(5)
Page 2, line 23 either “a” or use plural

You are correct.

Now we use plural: ...ground-based water vapor oscillations...

(6)
Line 1 on page 3- what is this supposed to mean?

We use a much longer data set than the campaign-based study of Li et al. (2007). As supposed to this study, we are able to derive monthly mean wave amplitude characteristics in the sub-diurnal period range. That was the main point we wanted to express in this sentence.

Due the substantial manuscript changes in the introduction, this sentence was removed. In the discusison part of the results (Sect. 4.3) we take up the study of Li et al. (2007) in context with the possible (we are not sure) observations of low frequency inertia-gravity waves in our data sets.

(7)
Line 24-25 on page 4: again, a poorly expressed thought: I think I understand why the winter data are more usable- due to lower tropospheric humidity. But this sentence implies something else. Do they mean that the measurement response in winter is sufficiently high that they can use a time integration as short as 3 hours (as opposed to say, a day?). If so they need to express that more clearly.

Yes, this sentence was not expressed very clearly. Due to a lower amount of tropospheric water vapor in winter the signal from the middle atmosphere is less attenuated and we can use a shorter integration time for the observed H_2O line spectrum at 22 GHz.

We now write: “During the winter months the tropospheric humidity is lower than during summer and in consequence the microwave signal from the middle atmosphere is

less attenuated by penetrating the troposphere to the ground-based receiver. Hence an integration of the signal of only 3 hours can be used to retrieve the H_2O profiles. A conceptional parameter that is usually used to express the altitude dependent measurement sensitivity is the so-called measurement response."

(8)
Page 5,line 10: "To our knowledge and made efforts," ? "made efforts" is poor English.

Ok, thank you for the grammatical hint.

This sentence is removed in section 2. We explain and show results of our "efforts" that try to show that our observed oscillations are not related to artificial effects and thus a real atmospheric phenomenon now in the beginning of the discussion of the results in Sect. 4.3.

(9)
Page 12, line 25 "is capable of resolving"

You are correct.

Changed "...is capable to resolve" to "...is capable of resolving"

3 Response to Referee #4

General remarks

(1)
Whereas the authors wrote in the introduction at page 5 lines 10–12 To our knowledge and made efforts, artificial effects leading to the observed 18-hour variability can be excluded and therefore the wave is expected to be of atmospheric origin. We aim to report on findings based on middle atmospheric observations and model simulations. Revealing possible sources of an 18-hour inertia-gravity wave is beyond the scope of this paper. However, in the following they are only focusing on an 18-hour inertia gravity wave based on a single case study (Figs. 12 and 13). From the reviewer point, this generalization on all events is not valid because the difference between the observed period (∼18 h) and the inertial period of 16.4 h as upper limit for the intrinsic period at the latitude of Bern (46.88°N) requires more or less at least constant background winds to get the Doppler shift of the intrinsic GW frequencies which has not been shown here.

The focus on the two wave events (with hodograph analysis) is removed by completely omitting the SD-WACCM data. The generalization from the 2 events was not valid. We

now only focus on our ground-based observations and let the explanation of the 18-hour wave open to some extent. In the discussion we now do not only focus on inertia-gravity waves but also on the possibility of a wave-wave interaction between the migrating diurnal tide and the quasi 2-day wave, which is a more likely explanation even in regard to the quite low vertical resolution of our microwave radiometers.

In the new Sect. 4.3 (Discussion) we add the argument about the background wind speed related to the inertia frequency: "...The main point would be to check if the vertical wavelengths are large enough for our microwave radiometer observations with a vertical resolution of more than 10 km to be able to see it. Further, in case of inertia-gravity waves with a ground related frequency of around 18 hours a specific background wind speed is required that reduces the actual intrinsic wave frequency (Doppler shifting) below the inertia frequency which is 16.44 h at the location of Bern."

(2)
An oscillation with a period of about 18 h can also be the result of a nonlinear wave-wave interaction of two waves, e.g. between quasi two day wave and the semidiurnal tide or between the semidiurnal and terdiurnal tide. This must be checked and considered as a possible reason for the obtained oscillations.

This is a very interesting hint. It could be that we observed a non-linear wave-wave interaction between the quasi 2-day wave and the migrating diurnal tide resulting in a westward traveling sum wave with periods around 16–18 hours, that behaves like a inertia-gravity wave (as stated in Lieberman et al. (2017)). So far we have not analyzed the quasi 2-day wave in our data for Bern, but this is planned in future. Within this paper revision it is virtually not possible for us to do this. In this paper we only focus on an interesting wave observation, but the clarification about the sources/causes has to be postponed.

We decided not only to discuss about our results in regard of inertia-gravity waves, but also in regard of such a non-linear wave-wave interaction in the new section 4.3 now. See also answer to major comment 1 by Referee #3.

(3)
In contrast to Figs 3 and 4, the SD-WACCM spectra show diurnal tidal waves with a poor spectral resolution, but no dominant oscillations between 15 and 21 h. It is surprising that there is such a similarity and significant correlation between the bandpass filtered wave amplitudes derived from MIAWARA and the corresponding water mixing ratio derived from SD-WACCM simulations (Figs 6–10). Can you comment this?

In Figure 10 only the correlations of individual amplitude profiles are shown. The plot somehow is misdirecting and does not show a temporal correlation between MIAWARA and SD-WACCM 18-hour amplitudes. We figured out, that the quite high correlation coefficients came from the good agreement between the model and observations at low

altitudes (below 0.1 hPa), where no or only very small 18-hour wave amplitudes are present.

Figure 10 is removed and a comparison between MIAWARA and SD-WACCM in terms of the 18-hour variability is not meaningful. Anyway the whole SD-WACCM part of the original manuscript is canceled.

(4)
Please explain and/or improve the spectral resolution presented in Figs 3–5.

In Sect. 4.1 (Monthly mean H_2O wave spectra) the spectral resolution is given as 1 hour. A even shorter spectral resolution does not make sense in our opinion because the sampling of the water vapor data is at 3 hour intervals. So the spectral resolution is already much shorter than the temporal resolution of the raw data.

Added the word "spectral" in Sect. 4.1 to make it more clear.

(5)
Please define the term "relative amplitudes" as used in Figs 6–10.

Thank you, it is important to make the term "relative amplitudes" more clear.

In the beginning of Sect. 4.2 (Temporal evolution of quasi 18-hour wave) we now write: "Absolute and relative wave amplitudes, which are calculated relative to the average water vapor mixing ratio at a pressure level over the investigated time period, are presented."

(6)
The case study (d) from 5–9 Dec 2015 (Fig 11) shows similar wave amplitudes between MIAWARA (water vapour), WIRA (u), and SD WACCM (u) and gives confidence that, with meridional winds from WIRA, a better wave estimation at the same location will be possible. In the frame of the used title focusing on 18 h waves, however, Fig. 4c show during this period only tides (12h, 24h) but nothing between 15–21 h

It is true that with meridional winds from WIRA a first estimation of the wave characteristic would be possible above the measurement site. The fact that our instrument see this wave leads also to the aspect that the 18-hour period waves must have a much larger vertical wavelength than the original stated range $\lambda_z < 6$ km. So to say, the SD-WACCM hodograph analysis resulted in impractical conclusions. The fact that Fig. 4c has no prominent amplitude peaks within the 15–21 h period range is due to the averaging over the entire month. The diurnal and semi-diurnal wave amplitudes were on average much larger in December 2015 than the 18-hour wave component. Unfortunately we can only use co-located WIRA data in December 2015 to compare with the water vapor observations.

Nothing changed accordant to the above comment 6.

(7)
The hodographs in Figs 13 and the derived possible characteristics of a monochromatic gravity wave are based on band pass filtered model simulations. It is not clear for the reviewer, how realistic are these simulated amplitudes, where the gravity waves are handled consistent a parametrization (see Page 6, lines 21–26). The cited papers of Baumgarten et al. (2015) and Li et al. (2007) used LIDAR data with a high resolution to estimate their hodographs. Please consider also a Stokes parameter analysis to get a more averaged GW description instead of the snapshot hodograph of a single monochromatic wave. Furthermore it is recommended to add the dispersion and Doppler equation to the wave parameter estimation to improve the readability.

We agree that the derived wave characteristics from filtered SD-WACCM simulations and their expressiveness was unclear in context to our observations. Probably other and more sophisticated model simulations (e.g. higher spatial resolutions) would be needed for a better comparison.

The complete hodograph analysis is not shown any more as stated before. Old Sect. 4.3.1 is removed and with it the numerical method part in Sect. 3 describing the hodograph method.

(8)
The AURA MLS temperatures and water vapour profiles are important for the MIAWARA data as described in Sec 2.1 (page 4). However, at altitudes of about 0.1 hPa, where the observed 18 h oscillations have their maxima, the vertical resolution lies between delta h 5.5 and 6 km (see page 6, line 6) , so that only waves with vertical wavelengths larger than 2 x delta h (11–12 km) can be resolved. From this point, the filtered temperature profiles with vertical wavelengths ¡ 6 km are questionable, at least above 0.1 hPa.

We agree that the filtered Aura MLS temperature profiles in regard of wavelengths below 6 km is problematic due to the too low vertical resolution.

We decided to completely remove the Aura MLS temperature analysis during the revision.

Technical corrections

(9)
Page 2 line 8 please add wind

Ok.

Page 2, line 8: We added “wind”

(10)
Page 7 line 13 bandpass

Ok.

Page 7, line 13: Changed “passband” to “bandpass”.

(11)
Page 8 line 32 are given in the next Section.

OK.

Sentence is removed because it pointed to SD-WACCM results.

References

Li, T., She, C.-Y., Liu, H.-L., Leblanc, T., and McDermid, I. S. (2007). Sodium lidar-observed strong inertia-gravity wave activities in the mesopause region over fort collins, colorado (41n, 105w). *J. Geophys. Res. Atmos.*, 112(D22). D22104.

Lieberman, R. S., Riggin, D. M., Nguyen, V., Palo, S. E., Siskind, D. E., Mitchell, N. J., Stober, G., Wilhelm, S., and Livesey, N. J. (2017). Global observations of 2 day wave coupling to the diurnal tide in a high-altitude forecast-assimilation system. *Journal of Geophysical Research: Atmospheres*, 122(8):4135–4149. 2016JD025144.

Nicolls, M. J., Varney, R. H., Vadas, S. L., Stamus, P. A., Heinselman, C. J., Cosgrove, R. B., and Kelley, M. C. (2010). Influence of an inertia-gravity wave on mesospheric dynamics: A case study with the poker flat incoherent scatter radar. *J. Geophys. Res. Atmos.*, 115(D3).

Quasi 18-hour wave activity in ground-based observed mesospheric H_2O over Bern, Switzerland

Martin Lainer[1], Klemens Hocke[1,2], Rolf Rüfenacht[1,3], and Niklaus Kämpfer[1,2]

[1]Institute of Applied Physics, University of Bern, Bern, Switzerland
[2]Oeschger Center for Climate Change Research, University of Bern, Bern, Switzerland
[3]Actual affiliation: Leibniz-Institute of Atmospheric Physics, Kühlungsborn, Germany

Correspondence to: M. Lainer (martin.lainer@iap.unibe.ch)

Abstract. Observations of oscillations in the abundance of middle atmospheric trace gases can provide insight into the dynamics of the middle atmosphere. Long term, high temporal resolution and continuous measurements of dynamical tracers within the strato- and mesosphere are rare, but would be important to better understand the impact of ~~planetary and gravity~~ atmospheric waves on the middle atmosphere. Here we report on water vapor measurements from the ground-based microwave radiometer MIAWARA located close to Bern during two winter periods of 6 months from October to March. Oscillations with periods between 6 and 30 hours are analyzed in the pressure range 0.02–2 hPa. Seven out of twelve months have the highest wave amplitudes between 15 and 21 hour periods in the mesosphere above 0.1 hPa. The quasi 18-hour wave signature in the water vapor tracer is studied in more detail ~~. We examine the temporal behavior and use SD-WACCM simulations for comparison and to derive characteristic wave features considering low-frequency gravity-waves being involved in the observed water vapor oscillations. The~~ by analyzing its temporal evolution in the mesosphere up to an altitude of 75 km. An 18-hour ~~wave is also found in SD-WACCM horizontal wind data and in measured zonal wind~~ oscillation in co-located zonal wind observations from the microwave Doppler wind radiometer WIRA ~~. For two cases in January 2016 we derive the propagation direction, intrinsic period, horizontal and vertical wavelength of the model resolved 18-hour wave. A south-westward to westward propagation with horizontal wavelengths of and intrinsic periods close to are found. Vertical wavelengths are below . We were not able to single out a distinct temporal correlation between~~ could be identified within the pressure range 0.1–1 hPa in December 2015. The origin of the observed upper mesospheric quasi 18-hour ~~band-pass filtered water vapor and wind data time series, although should mostly be dynamically controlled in the mesosphere and sub-diurnal time range. More sophisticated numerical model studies are needed to uncover the manifold effects of gravity waves on the abundance of chemical species~~oscillations is uncertain and could not be determined with our available data sets. Possible drivers could be low frequency inertia-gravity waves or a non-linear wave-wave interaction between the quasi 2-day wave and the diurnal tide.

1 Introduction

The dynamics of the middle atmosphere is controlled by a ~~manifold~~ broad spectrum of waves. Knowledge about the wave characteristics and incidence is important, not only to better understand the elements of middle atmospheric dynamics, but

carrying on to improve predictions of weather (Hardiman et al., 2011) and climate (Orr et al., 2010) models. Latter are getting more important since the social impact of severe weather events and climate change is increasing.

Waves with horizontal wavelengths reaching thousands of kilometers and showing periods up to several weeks are classified as planetary waves. A well-known class of planetary waves are Rossby waves (Salby, 1981b). Their periods range from 2 to approximately 18 days in the middle atmosphere, showing strong inter-annual variability (Jacobi et al., 1998). Investigations of the quasi 2-day wave are found for instance in studies by Salby (1981a); Rodgers and Prata (1981); Yue et al. (2012) and more recently by Tschanz and Kämpfer (2015). Latter , who analyzed the 2-day wave signatures in arctic middle-atmospheric water vapor measurements in conjunction with the occurrence of sudden stratospheric warmings. Characteristics of the 5-day wave were analyzed by Rosenlof and Thomas (1990); Wu et al. (1994); Riggin et al. (2006); Belova et al. (2008) and waves with even longer periods have been observed in the mesosphere and lower thermosphere (Forbes et al., 1995; McDonald et al., 2011; Scheiben et al., 2014; Rüfenacht et al., 2016).

Besides the presence of planetary waves, signatures of atmospheric tides (ter-diurnal, semi-diurnal, diurnal) can be seen in middle atmospheric constituents or parameters like wind, ozone, water vapor and or temperature. Diurnal tides can be triggered by latent heat release within the troposphere (Hagan and Forbes, 2002) and can be of migrating or non-migrating nature. Overall complex interactions of atmospheric waves and coupling processes between different atmospheric layers exist. As Forbes (2009) assessed, the semi-diurnal solar thermal tide is a feature in the atmosphere of the earth, and serves to globally couple the troposphere, stratosphere, mesosphere, thermosphere and ionosphere.

Regarding the variability of the solar radiation, two major regimes, the 11-year and 27-day solar cycle, can affect the chemical composition of the middle atmosphere. While signatures of the 27-day solar rotation cycle were found in mesospheric OH and (Shapiro et al., 2012; Lainer et al., 2016) and stratospheric and temperature (Ruzmaikin et al., 2007) , the 11-year variability is a profound feature for instance in stratospheric ozone and temperature. Labitzke et al. (2002) performed general circulation model (GCM) simulations to study the impact of the 11-year solar cycle on geopotential height and temperature and made comparisons to observations.

Besides Apart from direct observations of middle atmospheric wind as a proxy for dynamical patterns, it is common to use observations of H_2O or that can serve as diagnostic and dynamical tracers, even from ground-based profile measurements (Liu et al., 2013; Lainer et al., 2015), due to their relative long chemical lifetime, which is on the order of weeks in the mesosphere (Brasseur and Solomon, 2006).

Here we report on ground-based observed water vapor oscillation oscillations in the mesosphere above Switzerland (46.88 °N, 7.46 °W) with a period of around 18 hours and investigate the temporal and monthly mean characteristicsmonthly mean and temporal characteristics of the wave amplitudes. This is to our knowledge the first study that explores a quasi 18-hour dominant wave mode in wintry (Northern Hemisphere) upper mesospheric conditions with passive microwave radiometry techniques.

Literature indicates that the 18-hour oscillation in mesospheric water vapor could be connected to the presence of low-frequency gravity-waves (GW), also called inertia-gravity waves, of similar apparent period. Li et al. (2007) described an 18-hour inertia-gravity wave. They used sodium-lidar measurements to probe the atmosphere between 80 and . In a 80-hour lasting campaign (December 2004) observations of temperature, sodium density, zonal and meridional wind were conducted. A linear least

square data fitting revealed strong amplitudes in the wind fields with a characteristic increase with altitude. Wind amplitude peaks were detected between 96 and . The 18-hour signal was also present in temperature and sodium density, but less distinct. By applying linear wave theory, for details see e.g. Chapter 2 in Nappo (2002) , an estimation of the horizontal wave propagation direction (), wavelength (about) and phase speed () could be determined for the first time with experimental data from a single instrument (Li et al., 2007) .

We show with a much larger data set in which months the 18-hour or nearby period modes dominate in the water vapor profiles obtained by the Middle Atmospheric Water Vapor Radiometer (MIAWARA, Deuber et al. (2004)). The MIAWARA instrument has an upper measurement limit at approximately () and does not reach the same altitudes as a sodium-lidar system. The advantage of microwave radiometers is that they can measure during day and night and are not critically influenced by the occurrence of clouds whereas lidar instruments usually are.

Gravity waves are a natural feature of a stably stratified atmosphere, where the squared Brunt-Väisälä frequency $N^2 > 0$. In general, GW can be classified into three types, with either low, medium or high intrinsic wave frequencies $\hat{\omega}$ (Fritts and Alexander, 2003) . The role of atmospheric GW is to transport and deposit momentum by wave-breaking. Besides shear instability GW breaking events are an important source of turbulent kinetic energy production near the mesopause (Fritts et al., 2003) . As the sub-spectrum of gravity waves is large, plenty of different triggering mechanisms exist, including: Orographic lifting, spontaneous emission from jet streams and fronts, convective systems or water waves on oceans. Strong emissions of atmospheric gravity waves of low frequency (periods from a few hours to about 24 hours) were detected in the exit region of jets in the upper troposphere, as presented by Plougonven and Zhang (2014) and references therein. In the jet exit region the air flow is from north to south and establishes a force that decelerates the air when it leaves the jet streak (Shapiro and Keyser, 1990) . The vertical motion resulting from the described mechanism leads to rising air in the north quadrant and sinking air in the south quadrant of the jet streak system. For an inertia-gravity wave gravity/buoyancy is not the only restoring force. The Coriolis force needs to be considered, since the horizontal wavelengths can reach up to (Maekawa et al., 1984) with an estimated Rossby number $\mathrm{Ro} < 1$ of the flow system. A coherent low-frequency GW packet with vertical wavelengths between has been studied by Nicolls et al. (2010) . They suggest a geostrophic adjustment of the tropospheric jet stream a few days before the actual observation as the main triggering mechanism of the inertia-gravity wave packet.

In our study we use water vapor simulation data from the specified dynamics (SD) version of the Whole Atmosphere Community Climate Model (WACCM) for comparison with the ground-based observed water vapor oscillation. SD-WACCM wind and potential temperature fields are used to determine intrinsic period, horizontal propagation direction, horizontal and vertical wavelengths of the model resolved 18-hour inertia-gravity wave . As our research group at the Institute of Applied Physics (University of Bern) operates unique microwave radiometers to observe mesospheric zonal and meridional wind components (Rüfenacht et al., 2014) , we analyze wind measurements from October 2015 to March 2016 to investigate possible 18-hour wave events in the upper mesosphereradiometric techniques. For this investigation not only ground-based water vapor data is analyzed. Mesospheric zonal wind above Bern measured by the microwave Doppler wind radiometer WIRA (Rüfenacht et al., 2014) is also considered. The focus of this paper is on the observation of atmospheric wave signatures and their temporal evolution.

In Sect. 2 the data sets from the ground-based ~~measurements, model simulations and Aura MLS satellite observations~~ remote sensing instruments are described. The data processing methodology and the underlying numerical approach is part of Sect. 3. Section 4 describes and ~~analyses~~ analyzes the results and some distinguished features of the present 18-hour ~~wave oscillation (~~spectral component. Possible implications of the observed wave activity in our H_2O and wind data like an impact of inertia-gravity waves or a coupling of a quasi 2-day wave to the diurnal tide is addressed in Sect. ~~4.2) and implications are addressed. Concluding remarks~~ 4.3. Final conclusions are provided in Sect. 5.

2 ~~Data~~ Instruments and data sets

~~In this section we describe the instruments and numerical models used to evaluate and analyze the quasi 18-hour wave activity. Two ground-based microwave radiometers (retrieving water vapor or wind), the NASA operated EOS (Earth Observing System) Aura MLS (Microwave Limb Sounder) instrument and data from SD-WACCM simulations are explained.~~

2.1 ~~Ground-based microwave observations~~

The advantage of ground-based microwave radiometry is to continuously measure the amount of atmospheric trace gases at altitudes between roughly 30 and 80 km under most environmental conditions. Observations are possible during day, night and under cloudy conditions. The technique is widely used to study the middle atmosphere (Kämpfer et al., 2012). In this section we present the middle atmospheric water vapor radiometer MIAWARA and Doppler wind radiometer WIRA.

2.1 Middle atmospheric water vapor radiometer

The middle atmospheric water vapor radiometer MIAWARA was built in 2002 at University of Bern (Deuber et al., 2004) . The Front-End of the ~~MIAWARA instrument~~ radiometer receives emissions from the pressure broadened rotational transition line of the H_2O molecule ~~. The~~ at the center frequency of ~~the transition line is~~ 22.235 GHz. For studying oscillations with periods shorter than one day, a high temporal resolution of a few hours with an evenly spaced time series is required. In our case ~~the~~ a MIAWARA water vapor ~~time series has~~ retrieval version with a temporal resolution of 3 hours is applied. The H_2O retrieval from ~~3 hourly~~ the integrated raw spectra is based on the optimal estimation method (OEM) as presented in Rodgers (2000). We use the ARTS/QPACK software (Eriksson et al., 2005, 2011), where the OEM is used to perform the inversion of the atmospheric radiative transfer model ARTS. The FFT (Fast-Fourier Transform) spectrometer ~~at~~ in the Back-End of MIAWARA has a resolution of 60 kHz and the retrieval ~~takes~~ uses an overall spectrum bandwidth of 50 MHz. A monthly mean zonal mean Aura MLS climatology provides the a priori water vapor profile and additionally Aura MLS is used to set the pressure, temperature and geopotential height in the retrieval part. MIAWARA is part of NDACC (Network for the Detection of Atmospheric Composition Change) and is persistently probing middle atmospheric H_2O from the Atmospheric Remote Sensing observatory in Zimmerwald (46.88 °N, 7.46 °E, 907 m a.s.l.) close to Bern since 2006. In the stratosphere the vertical resolution of the water vapor profiles is 11 km and degrades to about 14 km in the mesosphere (Deuber et al., 2005). A recent

validation against the Aura MLS v4.2 water vapor product (Livesey et al., 2015) revealed that for most months and altitudes the relative differences between MIAWARA and Aura MLS are below 5 % (Lainer et al., 2016).

As our water vapor retrieval uses a fixed 3-hour integration , the measurement response (MR) in the mesosphere is sufficiently high during months from October to March/April. During the winter months the tropospheric humidity is lower than during summer and in consequence the microwave signal from the middle atmosphere is less attenuated by penetrating the troposphere to the ground-based receiver. Hence an integration of the signal of only 3 hours can be used to retrieve the H_2O profiles. In order to define a reliable altitude range for the retrieved data, the area of the averaging kernels (the so-called measurement response) is a good indicator. A typical used threshold value range for the measurement response indicator is between 60–80 %.

The MIAWARA H_2O time series between October 2014 and March 2016 is shown in Fig. 1 and the MR criterion with a measurement response of 80 % that is represented by the white horizontal lines. Except for some outliers we consider the upper measurement limit to range within 0.02–0.04 hPa during the NH winter seasonwinter time period. In the summer season , when the humidity in the troposphere is high, our the H_2O retrieval from an 3 hour integration time signal integration has a significant lower measurement response. It is not possible to get information that is sufficiently a priori independent above approximately 0.1 hPa in the upper mesosphere. We anticipate that all additional MIAWARA related plots will not show upper and lower measurement limits due to the fact that any a priori contribution cannot have an effect on a sub-diurnal variability as it is not resolved in the used seasonal climatological data. Further we note that we miss 1 one week of MIAWARA data due to hardware problems beginning in the end of December 2015. This data gap pops up as is shown by a white bar in the MIAWARA H_2O time series.

Local instrument related temperatures at the MIAWARA measurement site, such as outdoor temperatures, indoor temperatures, mixer temperatures, Aquiris FFT FPGA (Field Programmable Gate Array) temperatures, hot-load and receiver temperatures, have been analyzed for oscillations that could have an influence on the observed wave signatures in the retrieval data. The individual temperature amplitudes were examined for several months. Local peaks in the monthly mean amplitude spectra occur close to 24 and 12 hours due to insolation.No distinct amplitude peaks have been found in the period range between 15 and 18 hours. Additionally the atmospheric opacity at obtained from tipping curve measurements and the measurement response in the water vapor retrieval were examined by the same filter algorithms for waves with periods between 6 to 30 hours. No correlations to the wave spectra or prominent amplitude peaks between 15 and 21 hours were found during months when a distinct 18-hour wave was existent in the MIAWARA data.

To our knowledge and made efforts, artificial effects leading to the observed 18-hour variability can be excluded and therefore the wave is expected to be of atmospheric origin. We aim to report on findings based on middle atmospheric observations and model simulations. Revealing possible sources of a In order to provide more information on the water vapor variability in the upper mesosphere, Figs. 2 and 3 are shown. There the monthly water vapor time series of MIAWARA averaged between 0.02–0.1 hPa are plotted during the two winter time periods. It is the same altitude region where the 18-hour inertia-gravity wave is beyond the scope of this paperoscillations appeared. Later in the spectral wave analysis monthly mean wave spectra of the same months will be derived.

2.2 Doppler wind radiometer

In 2012 the novel wind radiometer WIRA (Rüfenacht et al., 2014) has been developed at the Institute of Applied Physics at the University of Bern. It is the only instrument capable to steadily observe wind in the otherwise sparsely probed atmospheric layer between 35 and 70 km altitude. Other techniques like rocket based meteorological measurements (Schmidlin, 1986) can provide data in this region but suffer from high operational costs, that makes them suitable for short campaigns but not for continuous observations. WIRA, a ground-based passive microwave heterodyne receiver, observes the Doppler shifts of the pressure-broadened emission line of ozone at 142 GHz. ~~As for MIAWARA, the~~ The retrieval of zonal and meridional middle atmospheric wind components is based on OEM. The measurement uncertainty ranges from 10 to 20 m s^{-1} and the vertical resolution varies between 10 and 16 km. For more detailed information about the instrument we ~~point the reader~~ refer to papers by Rüfenacht et al. (2012, 2014). In order to resolve the 18-hour wave the retrieval was pushed to the limits by using measurements with an integration time of 6 hours only, instead of the usual 24-hour averages. Therefore, a new retrieval version which improves the wind accuracy of the mesospheric wind estimates has been used in this study. The WIRA instrument ~~is capable to resolve~~ measured the quasi 18-hour wave over Bern in the zonal wind vector component for only ~~short time periods~~ a short time period between 2015-12-05 and 2015-12-09 in the pressure range 0.1–1 hPa. ~~One of these time periods is between 2015-12-05~~ Figure 4 shows zonal wind data set as measured by WIRA between 2015-12-02 and ~~2015-12-09, and Fig. ?? shows the corresponding zonal wind profile time series~~2015-12-15. In the whole altitude domain the measurement response of the WIRA radiometer is greater than 0.8.

2.3 ~~EOS Aura MLS satellite observations~~

~~Space-borne temperature observations are often used to investigate gravity wave activity (Ern et al., 2004; Hocke et al., 2016) . With incorporating MLS temperature data in the study we strive to confirm and supplement the wave signatures in and wind profile data. Two case studies of the SD-WACCM resolved 18-hour inertia-gravity wave revealed vertical wavelengths below (Sect. ??). Therefore, temperature profiles from the Aura MLS satellite instrument are used to search for oscillations with vertical wavelengths smaller than . Oscillations in temperature profiles are helpful to identify local vertical structures associated with inertia-gravity waves. Increasing wave periods and horizontal wavelengths typically lead to decreasing vertical wavelengths as it can be deduced from the dispersion relation for inertia-gravity waves (Fritts and Alexander, 2003) .~~

~~For the location of Bern usually two temperature profiles per day are available in the Aura MLS data set. The vertical resolution in temperature profiles from MLS v4.2 is between and . It increases to at and decreases to at . At higher altitudes the dropping in vertical resolution is ongoing and reaches values of (), respectively () (Livesey et al., 2015) . A vertical interpolation to a grid was applied to fulfill the Nyquist-Shannon sampling theorem. The along track resolution of the temperature measurements is about within the pressure range .~~

2.3 ~~SD-WACCM model simulations~~

In our study the CESM (Community Earth System Model) v1.2.2 model version is used. It couples sub-models of the atmosphere, land, ocean and sea ice. The whole atmosphere model, called WACCM (Marsh et al., 2013) is a capacity of CAM (Community Atmosphere Model) v4 (Collins et al., 2006) . Our simulations make use of the specified dynamics atmosphere model version SD-WACCM, whereby the model becomes nudged by 6-hourly GEOS5 (Goddard Earth Observing System 5) meteorological analysis data (horizontal winds, temperature, surface pressure, surface wind stress, latent and sensible heat fluxes) every internal model time step interval of 30 minutes (Kunz et al., 2011; Lamarque et al., 2012) . The nudging rate linearly decreases from below to between . A horizontal grid resolution of (latitude) and (longitude) is specified. Overall, 88 atmospheric layers up to with a resolution range between exist. The vertical coordinates are of hybrid sigma-pressure kind and follow the terrain near the surface whereas a transition to pure pressure coordinates takes place up to an altitude of approximately . The chemistry module of SD-WACCM is based on MOZART (Model for OZone and Related chemical Tracers, Emmons et al. (2010)).

As described by Lin and Rood (1997) , gravity waves are handled explicitly in a way consistent to the semi-Lagrangian advection scheme. A numerical scheme revealed by McFarlane (1987) is used to parameterize GWs triggered by orography. Gravity waves emerging from other sources and their propagation is implemented according to a scheme of Lindzen (1981) , given that convection is the main initiation mechanism. The use of more parameterization schemes to cover non-resolved GW sources can significantly improve the model performance within the stratosphere in regard of a better representation of observed dynamical variability (Limpasuvan et al., 2012) .

We use the SD-WACCM simulation output for one grid point that represents our measurement location of Bern (,). The following model variables are processed: Water vapor volume mixing ratio, potential temperature, zonal u and meridional v wind components (nudged). Every hour a data value is available on each vertical grid point. On the one hand oscillations in SD-WACCM water vapor and wind, which have periods close to 18 hours, are investigated and on the other hand the potential temperature is used to compute the Brunt-Väisälä frequency N (Eq. (**??**)) together with the perturbation time series u' , v' to apply the hodograph method (Sawyer, 1961) in order to determine model resolved inertia-gravity wave characteristics.

$$N = \sqrt{\frac{g}{\Theta}\frac{\partial \Theta}{\partial z}}$$

3 Numerical methodsmethod

In order to derive the wave spectrum in the MIAWARA and SD-WACCM of the MIAWARA H_2O data time seriesfor Bern, we applied the following numerical methods: A digital band-pass filter (non-recursive finite impulse response) with a comprised Hamming window is applied to MIAWARA and SD-WACCM data the data time series to extract amplitudes of hidden oscillations of periods between 6 and 30 hours. Performing windowing methods to measurement time series ensure that the data endpoints fit together and smooth out short-term fluctuations to put longer-term cycles to foreground. Therefore the spectral leakage can be reduced (Harris, 1978). In Studer et al. (2012) the numerical structure of the band-pass filter has been shown. Lately the filter has been used to investigate the impact of the 27-day solar rotation cycle on mesospheric water vapor (Lainer

et al., 2016) and to analyze the quasi 16-day planetary wave during boreal winter (Scheiben et al., 2014). We follow the advice from Oppenheim et al. (1989) and run the filter with a zero phase lag forward and backward along the measurement and simulation time series. The cut-off frequencies of the ~~passband~~ bandpass attenuation are either set to 5 % or 16.6 % (depending on the analysis method) of the initialized central frequency. The central frequency prearranges the size of the Hamming window which is the triple-fold of the central period. Our filter and window setup guarantees a fast adaptability to data variations in time. ~~In order to show how the 18-hour wave amplitudes appear in SD-WACCM compared to the MIAWARA water vapor analysis, a time dependent Pearson product-moment correlation coefficient (PPMCC) is computed.~~

~~In general the application of hodograph method in an atmospheric environment where single monochromatic gravity waves appear is valuable for obtaining intrinsic frequencies, propagation directions and as a result the horizontal wavelengths λ_h . Quite large uncertainties can however occur by estimating λ_h , as shown by Zhang et al. (2004) . But they note that for inertia-gravity waves with short vertical wavelengths the uncertainties become smaller. A substantial number of gravity wave studies (Li et al., 2007; Plougonven and Teitelbaum, 2003; Baumgarten et al., 2015) made use of the hodograph analysis.~~

~~A fitted hodograph ellipse from the wind perturbation amplitudes (u' , v') will rotate clockwise with increasing altitude for the Northern Hemisphere (Tsuda et al., 1990) , pursuant to the polarization relation (Eq. (**??**)), if the analyzed inertia-gravity wave has a phase velocity tending downwards.~~

$$u' = \left(\frac{i\hat{\omega}k - fl}{i\hat{\omega}l - fk} \right) v'$$

~~The wave phase propagation has a direction given by the vector (k,l,m) . The intrinsic frequency $\hat{\omega} = \omega - k\bar{u} - l\bar{v}$ is the frequency that would be observed while moving with the background wind $(\bar{u},\bar{v})$ (Fritts and Alexander, 2003) . The intrinsic frequency can be obtained from the hodograph ellipse by calculating the ratio between the major and minor axis ε according to $\hat{\omega} = \varepsilon \cdot f$, where f is the inertial frequency. Further, the inertial period can be easily calculated with $T_f = 2\pi f^{-1}$. The GW direction of horizontal propagation φ is determined by the orientation of the major ellipse axis. For now, two possible propagation directions exist. Tsuda et al. (1990) show how an explicit solution can be identified. The relation between the vertical and zonal wind perturbation velocities~~

$$\frac{w'}{u'} = -\frac{k}{m}$$

~~where k and m are the wave numbers in horizontal and vertical direction, can be used to clarify the GW horizontal propagation orientation. Since k is positive and m negative if the GW propagation consists of a downward phase velocity, the vertical wind perturbation of the gravity wave has to be upward. As soon as the GW propagation direction φ and intrinsic frequency $\hat{\omega}$ are known, Doppler relation and the dispersion relation for inertia-gravity waves can be applied to calculate the vertical and horizontal GW wavelengths λ_z and λ_h (e.g., Fritts and Alexander, 2003; Liu and Meriwether, 2004) .~~

~~In this context it is important to mention that an apparent wave frequency ω is larger than the intrinsic frequency $\hat{\omega}$ if the wave is moving in the direction of the air flow. It can be expressed with the Doppler relation ($\hat{\omega} = \omega - 2\pi\lambda_h^{-1}U_k^{-1}$), where~~

~~U_k is the horizontal wind speed in direction of wave propagation. In simplified terms, the Coriolis dependent dispersion relation can be wrapped up as~~

~~$$\hat{\omega}^2 = \frac{N^2 \cdot \lambda_z^2}{\lambda_h^2} + f^2$$~~

4 Results

4.1 Monthly mean H_2O wave spectra

A mean wave amplitude is obtained by averaging amplitude series over time. For example, a final H_2O wave amplitude spectrum as presented in Fig. 5 and 6 is created by computing the monthly-averaged amplitudes as a function of the period. The period range goes from 6 to 30 hours with a spectral resolution of 1 hour. Overall, 12 months of microwave radiometric water vapor measurements were processed. The mean amplitude wave spectra reveal that except for October 2014 the highest wave amplitudes are located in the 18-hour period band for the 2014/15 period. During October 2014 a different regime close to a 12 hour period is dominating. Below 1 hPa amplitudes in water vapor are small. Regarding the 18-hour variability the altitude domain above 0.1 hPa is most interesting. During the 2015/16 period clear 18-hour signals can be found in November 2015, January and February 2016 (Fig. 6). During the other 3 months (October and December 2015, March 2016) high amplitudes show up with periods near 12 and 24 hours (tidal patterns). Clear and high wave amplitudes at exactly 18 hours are found in December 2014 (Fig. 5c), January 2016 (Fig. 6d) and February 2016 (Fig. 6e). The altitude region, where the 18-hour oscillation is prominent, is mostly above 0.1 hPa. We find monthly mean quasi 18-hour H_2O amplitudes in the range 0.2 5–0.35 ppm. Prominent wave events with sharp 18-hour periods happened in January and February 2016. ~~In the following the focus is put on these events. Monthly mean spectra as derived from SD-WACCM are presented in Fig. **??**. The SD-WACCM simulation data show no clear amplitude maximum in the period band as MIAWARA observations do. Nevertheless amplitudes of 0.15 to are present above . For the analysis of the SD-WACCM mean wave spectrum a sampling rate of 2 hours was applied.~~ Within the subsequent section we investigate how often the 18-hour wave packets have been observed in the MIAWARA water vapor time series. ~~Comparisons to SD-WACCM results are given.~~

4.2 ~~Quasi~~ Temporal evolution of quasi 18-hour wave~~characteristics~~

We present the whole temporal evolution (12 months) of the water vapor oscillations in the quasi 18-hour period band for MIAWARA~~and SD-WACCM as comparison. For all the comparisons with the numerical simulations we have to be aware of the fact that parameterized gravity-wave effects in models are generally considered poorly constrained by observations (Fritts and Alexander, 2003) .~~

~~For January 2016 we perform two hodograph analysis with SD-WACCM to show exemplary how the quasi 18-hour wave characteristics is resolved in the numerical model. Since WIRA has not been capable to derive meridional winds with high quality from October 2015 to March 2016 in Bern, it cannot be used jointly with SD-WACCM for the hodograph method. Instead, we concentrate on the temporal 18-hour wave amplitude in zonal wind in the case of WIRA data between 5th and 9th~~

~~of~~ . Absolute and relative wave amplitudes, which are calculated relative to the average water vapor mixing ratio at a pressure level over the investigated time period, are presented. A short period of 4 days in December ~~2015.~~ 2015 is used to compare the observed water vapor oscillations with co-located measurements of zonal wind oscillations with a similar spectral component of 18 hours.

4.2.1 ~~Temporal behavior~~

Both the absolute and the relative amplitudes of the 18-hour wave in the MIAWARA observations show that this wave occurs quite regularly during the investigated winter months (Figs. 7 and 8). The amplitudes of the wave become highest above the mid-mesosphere (0.1 hPa). ~~This is in quite good agreement with the SD-WACCM analysis (Figs. ?? and ??).~~ Local (in time) amplitudes reach up to 0.5 ppm or 12 % in relative units. Scheiben et al. (2013) showed that in the altitude range from 3 hPa to 0.05 hPa the diurnal H_2O amplitudes do not exceed 0.05 ppm. ~~Any kind of interference of migrating tides is not expected to produce water vapor amplitudes as large as observed for the quasi 18-hour wave. A comparative high difference by a factor of ten is present between MIAWARA diurnal and quasi~~ The 18-hour ~~wave amplitudes. The~~ H_2O wave ~~emergence takes place in packets , what is reminiscent of inertia-gravity waves. A growing of 18-hour wave~~ emerges in packets and a growing of the amplitudes with decreasing pressure ~~is observed and likewise supports an involvement~~ can be identified. Both wave characteristics could be reminiscent of inertia-gravity waves. ~~Correlation coefficients of vertical amplitude profiles of the quasi~~ But since the 18-hour ~~wave between MIAWARA and SD-WACCM are given in Fig. ??. Regarding the time period over 12 months in total, the correlations can reach up to about 0.8 with confidence~~period exceeds the inertia period for the location of Bern by about 1.5 h some background wind speed is required that adjusts a lower intrinsic wave period to the 18-hour period observed from ground via Doppler shifting.

From October 2015 to March 2016 WIRA has observed middle-atmospheric wind over Bern. The 6 hourly binned WIRA data often show larger gaps of a few days in the time series at the altitudes of interest. This makes it difficult to search for 18-hour wave activity, when continuous measurements are necessary. During the highly dynamic phase at the beginning of December 2015 WIRA data with the required quality are available to complement the water vapor data. Continuous WIRA observations between 5th to 9th of December 2015 reveal a strong zonal 18-hour wave component (Fig. 9b). At the 5th and 8th of December the band-pass filtered absolute wave amplitudes reach values between 40 and 50 $m\,s^{-1}$. From 7th towards the 9th of December the zonal wind as observed by WIRA (Fig. ~~??~~4) is significantly accelerating. Between 0.3–0.7 hPa horizontal wind speed patterns almost double.

The observation of high ~~wave amplitudes~~ amplitudes of the zonal wind do not reach pressure levels below 0.3 hPa during the first event (5th of December). The second event (8th of December) shows high amplitudes almost covering the whole WIRA altitude range from 0.1–1 hPa. ~~By comparing the WIRA quasi 18-hour wave amplitude time series to SD-WACCM results (Fig. 9c) we find similar activity patterns. However, there are also significant differences. Most strikingly the SD-WACCM 18-hour zonal wind amplitudes are by a factor of 2 lower than that of WIRA.~~ The second event is not represented below 0.2 hPa. ~~However, the vertical differences between observations and model might to some part also be due to the limited vertical resolution of the instrument smearing out features in altitude.~~

In the MIAWARA water vapor data ~~the same~~ comparable 18-hour wave events on 5th and 8th of December ~~reach 18-hour oscillation amplitudes of~~ are present and absolute amplitudes of the oscillations reach about 0.35 ppm and 0.45 ppm. For the ~~wave~~ event on 8th of December 2015, the ~~pressure level of the amplitude maximum (~~overall altitudes where the wave amplitudes maximize (0.05–0.2 hPa) is in agreement between MIAWARA and ~~SD-WACCM. For WIRAthe maximum is located a bit lower in altitude (at)~~WIRA. The H_2O amplitude maximum for the first event is located at higher altitudes than ~~for WIRA and SD-WACCM winds~~the one for the zonal wind. The temporal extension ~~and behavior~~ of the 18-hour wave activity appears to agree ~~better with WIRA than with SD-WACCM~~quite well between the water vapor and zonal wind analysis.

~~An interesting periodoccurred in January 2016. A distinct~~ In the first part of the next Sect. 4.3 we will expand on possible MIAWARA instrument and retrieval artifacts that might have an influence on our data variability in the sub-diurnal time period. In conclusion we straighten out that the observed oscillations are robust. Later we discuss the results given in Sect. 4 in context to other performed studies related to inertia gravity wave activity and non-linear wave-wave interactions in the winter mid-latitude middle atmosphere.

4.3 Discussion

A spectral analysis of local instrument related temperatures at the MIAWARA measurement site, such as outdoor temperatures, indoor temperatures, mixer temperatures, Aquiris FFT FPGA (Field Programmable Gate Array) temperatures, hot-load and receiver temperatures, has been performed to see whether similar prominent 18-hour ~~water vapor amplitude at is found, that is higher (by) than the diurnal amplitude signature at (~~oscillations are present with a possible influence on the observed wave signatures in the H_2O retrieval data. The individual temperature amplitudes were examined for several months. Figure 10 shows the monthly mean temperature amplitudes for the six different parameters in January, February and March 2016. As illustrated in Fig. 6 ~~d). In particular the focus is put on 10 days between 2016-01-16 and 2016-01-26. Figure ?? presents the 18-hour band-pass filtered amplitude time series of MIAWARA~~ high wave activity with periods between 15 and 21 hours were seen in January and February 2016 but not in March 2016. Local peaks in the monthly mean amplitude spectra occur close to 24 and ~~SD-WACCM zonal and meridional wind vector components. The water vapor amplitudes are highest in the pressure range and reach about (Fig. ??a). During the presented 10 days, 3 periods of higher wave activity are detected: 2016-01-16 to 2016-01-18~~ 12 hours for $T_{Outdoor}$, ~~2016-01-20 to 2016-01-21 and 2016-01-22 to 2016-01-25 . The computed horizontal wind component wave amplitudes of the nudged model simulations (Fig. ??b and c) reach up to , but time of the amplitude maximums are different to those of~~ T_{Indoor}, T_{Mixer}, T_{FPGA} and T_{Hot} representing the diurnal temperature cycle. A typical value for the receiver temperature T_{Rec}, which is a parameter for the internally generated noise power of the MIAWARA receiver, is in the order of 160 K and the monthly average amplitude variability between the investigated periods is below 2 K. No distinct and strong variability can be identified in the period range between 15 and 18 hours for all temperature parameters that might effect the measured H_2O ~~. In~~ line spectrum at 22.235 GHz. The atmospheric temperature profile that is used in the retrieval calculation as a forward model parameter is a 3 day average profile calculated from Aura MLS observations and thus cannot generate any regular perturbations at 18-hour time intervals to our retrievals. Another parameter that is needed for the calibration of the H_2O radiometer is the cold sky brightness temperature which is dependent on the opacity. The atmospheric opacity at 22.235 GHz

is obtained from a tipping curve iteration according to Han and Westwater (2000) and was also analyzed for oscillations but only semi-diurnal and diurnal variations were found which is not unusual and related to changes in tropospheric humidity. Further, we use a seasonal varying Aura MLS H_2O climatology as water vapor a priori information, that also cannot influence the observed H_2O oscillations. In context to the a priori information we looked into oscillations of the a priori contribution A_c in the ~~case of the 2016-01-20 maximum in the zonal wind amplitude maximum occurs 12 hours later roughly at the same altitude~~ water vapor data over the whole altitude range of the radiometer (0.01–10 hPa). As example we show the spectral bandpass analysis for the same three months in the beginning of the year 2016 ~~(). For 2016-01-20 and 2016-01-20 we perform the propagation analysis (black vertical lines in~~ Fig. ~~??)as described in Sect. 3.~~

4.3.1 ~~Propagation analysis~~

~~The~~ 11). In January and March 2016 there are quite strong mean amplitudes of up to 10 % visible above 0.1 hPa, but the peaks are clearly outside of the quasi 18-hour ~~inertia-gravity wave, represented by the SD-WACCM model wind perturbations, is characterized by a hodograph analysis on 2016-01-20 and 12 hours thereafter (Fig. ??a and b). During these times the 18-hour oscillation appears in the MIAWARA water vapor data . The clockwise rotation of the u'/v' hodograph with rising altitude means that the wave is propagating upwards and its phase progression is downwards.~~ period band. Compared to the MIAWARA H_2O amplitude spectra no obvious correlation can be identified for the 3 months.

~~The horizontal wave propagation on 20th January is heading towards southwest at and veers westward to 12 hours later. The unambiguous direction along the main ellipse axis is determined by the vertical wind perturbation profiles (Fig. ??c and d) associated to~~ Many parameter tests were performed to see whether a similar 18-hour variability could contaminate the data retrieval of the MIAWARA instrument and lead to artificial effects. This can be excluded and therefore the observed oscillations in water vapor are expected to be a real atmospheric feature. Since the focus of the paper is on water vapor we will not expand the parameter tests on the wind retrieval here. Next, a short review on possible explanations for the quasi 18-hour ~~oscillation (Tsuda et al., 1990) . The horizontal wavelengths λ_h are estimated from the Doppler relation to be about , respectively . Intrinsic wave periods are close to 14 hours. These SD-WACCM model related findings are in general agreement to observational results of an~~ wave will be given.

As mentioned in Li et al. (2007) , the 18-hour oscillation in mesospheric water vapor could be connected to the presence of low-frequency gravity-waves (GW), also called inertia-gravity waves, of similar apparent period. In general, gravity waves are a natural feature of a stably stratified atmosphere, where the squared Brunt-Väisälä frequency $N^2 > 0$. Gravity waves can be classified into three types, with either low, medium or high intrinsic wave angular frequencies $\hat{\omega}$ (Fritts and Alexander, 2003) . The role of atmospheric gravity waves is to transport and deposit momentum by wave-breaking. Besides shear instability, breaking events are an important source of turbulent kinetic energy production near the mesopause (Fritts et al., 2003) . As the sub-spectrum of gravity waves is large, plenty of different triggering mechanisms exist, including: Orographic lifting, spontaneous emission from jet streams and fronts, convective systems or water waves on oceans. Strong emissions of atmospheric gravity waves of low frequency (periods from a few hours to about 24 hours) were detected in the exit region of jets in the upper troposphere, as presented by Plougonven and Zhang (2014) and references therein. A coherent 10.5 h low-frequency

GW packet with vertical wavelengths between 4–10 km has been studied by Nicolls et al. (2010) . They suggest a geostrophic adjustment of the tropospheric jet stream a few days before the actual observation as the main triggering mechanism of the inertia-gravity wave packet.

Li et al. (2007) described an 18-hour ~~oscillation with horizontal wavelengths of~~ inertia-gravity wave. They used sodium-lidar measurements to probe the atmosphere between 80 and 110 km. In a 80-hour lasting campaign (December 2004) observations of temperature, sodium density, zonal and meridional wind were conducted. A linear least square data fitting revealed strong amplitudes in the wind fields with a characteristic increase with altitude. Wind amplitude peaks were detected between 96 and 101 km. The 18-hour signal was also present in temperature and sodium density, but less distinct. By applying linear wave theory, for details see e.g. Chapter 2 in Nappo (2002) , an estimation of the horizontal wave propagation direction (245 °), wavelength (about 1800 km~~in the altitude range (Li et al., 2007) . A similar direction of wave propagation is likewise present.~~

~~The mean Brunt Väisälä frequency N () is determined by the potential temperature profiles and is used together with U_k , the wind speed projected onto the k -direction of the wave, to estimate the associated vertical wavelengths λ_z . For the presented case in Fig. **??**a (b), the mean U_k value between is () which leads to vertical wavelengths of roughly . Persistent~~) and phase speed (28 m s^{-1}) could be determined for the first time with experimental data from a single instrument (Li et al., 2007) . The vertical wavelengths were estimated to be between 15–18 km below an altitude of 97 km. The upper measurement limit of the MIAWARA water vapor radiometer is approximately at an altitude of 75 km (0.02 hPa) and does not reach the same altitudes as the previous mentioned sodium-lidar system. Still the vertical resolution of our instruments would be high enough to capture inertia-gravity ~~wave signatures in the middle atmosphere above northern Norway were studied by Baumgarten et al. (2015) and apparent vertical wavelengths between occurred. The given information about an intrinsic period of an identified monochromatic wave is 9.4 hours, which is 4 hours shorter than for our shown example.~~ waves with vertical wavelengths of about 20 km or larger. An advantage of microwave radiometers is that they can measure during day and night in a continuous operating mode and are not critically influenced by the occurrence of clouds whereas lidar instruments usually are.

~~Common vertical wavelength of less than of the~~ Revealing the possible observation of an 18-hour ~~wave initialized the idea to analyze Aura MLS vertical temperature profiles with respect to oscillations with similar wavelengths~~ inertia-gravity wave in our measurements would require more co-located atmospheric profile measurements of both zonal and meridional wind and temperature. ~~One intention is the identification of potential sources of the quasi 18-hour oscillation in middle atmospheric water vapor. In the following Sect. **??** a closer look at vertical middle atmospheric temperature anomalies over Bern is given.~~ The main point would be to check if the vertical wavelengths are large enough for our microwave radiometer observations with a vertical resolution of more than 10 km to be able to see it. Further, in case of inertia-gravity waves with a ground related frequency of around 18 hours a specific background wind speed is required that reduces the actual intrinsic wave frequency (Doppler shifting) below the inertia frequency which is 16.44 h at the location of Bern.

4.4 ~~Aura MLS temperature profiles~~

~~Aura MLS v4.2 temperature limb sounding profiles close to~~ In principle it would be possible to apply the hodograph method (Sawyer, 1961) with wind data from the WIRA radiometer and derive inertia-gravity wave parameters. During the time period

when the WIRA data was analyzed for this study the instrument was not able to provide meridional winds with sufficient high quality. Thus we were not able to derive hodographs in the upper mesosphere. We note, that a substantial number of gravity wave studies (Li et al., 2007; Plougonven and Teitelbaum, 2003; Baumgarten et al., 2015) made use of the ~~location of Bern are high-pass filtered in vertical direction. The objective is to see whether effects of low frequency inertia GW activity can be detected and whether they are in agreement with our previous given results. The key figure we present here is the development of temperature amplitudes ΔT_{HF} between from high-pass filtered temperature profiles at a cut-off vertical wavelength of . Since is the vertical resolution limit of MLS in the middle atmosphere, shorter wavelengths cannot be resolved.~~ hodograph analysis.

A Doppler wind and temperature lidar measurement campaign in northern Norway by Baumgarten et al. (2015) identified a number of inertia-gravity wave cases at altitudes between 60–70 km with emphasis on upward propagation and ~~λ_z~~ vertical wavelengths in the range 5–10 km. One observed ~~GW~~ gravity wave had an apparent period of approximately 11 hours. ~~For higher GW periods, e.g. 18 hours from our reported results, even smaller vertical wavelength have to be expected and we decided to take $\lambda_z < 6\,\mathrm{km}$ as the high-pass cut-off criterion~~Such a gravity wave could not be observed with our microwave radiometers due to a too low vertical resolution.

~~The analysis of Aura MLS temperature data makes use of two measured temperature profiles per day in proximity to the MIAWARA water vapor observation site . We show the two time periods as for the temporal investigation of the 18-hour wave activity (Sect. 4.2). The two covered 6 months periods in 2014/2015 and 2015/2016 are included. Figure **??** shows vertical as well as temporal temperature structures in the atmosphere induced by low frequency gravity waves. Wavelike disturbances in time occasionally occur below showing higher temperature amplitudes up to , for instance between 2014-12-27 and 2015-01-16 or the week around 2015-12-22. A prominent feature for both time periods is a band-like structure between roughly () with more or less consistently high ΔT_{HF} amplitudes. Pronounced quasi~~ A dynamic feature of the winter time mid-latitude mesosphere is the polar vortex. Since large meridional gradients in tracer concentrations exist across the vortex edge, it could be that a regular movement of the vortex edge above an observation site triggers an oscillation in an atmospheric trace gas such as H_2O. Indeed we find such oscillations of the polar vortex edge during winter above Bern, but the dominant period is 24 h in the mesosphere (0.01–1 hPa). We could not find any connection to an 18-hour ~~MIAWARA water vapor wave activity is found within or close to the observed band-like structure of large temperature oscillations.~~

~~The wave propagation beyond an altitude of seems to be suppressed for longer time periods. Irregularly and during rather short periods waves are able to travel further upwards. The time range 2015-12-18 to 2015-12-26 is an example when low frequency gravity waves with $\lambda_z < 6\,\mathrm{km}$ were observed throughout the middle atmosphere (Fig. **??**b), since wave dissipation and reflections were suppressed.~~

~~The vertical propagation is very sensitive to the actual atmospheric background wind conditions. As Charney and Drazin (1961) show, the reflection of planetary waves due to wind shear in the middle atmosphere is a prevailing atmospheric process. Further an environment of high wind shear favors the elimination of a fraction from any present atmospheric gravity wave spectrum (Hines and Reddy, 1967) .~~ period we are focusing on in this study.

~~Broadly speaking, a suppression of wave dissipation and reflection processes can be linked to wind shear properties in different atmospheric layers. One commonly used variable to reflect speed and directional shear is the bulk shear vector that can be obtained from the conventionally used u /v hodograph. The bulk shear vector is figured out by the subtraction of the two relative to ground wind vectors at~~ Besides the potential observation of inertia-gravity wave activity in our presented H_2O and zonal wind data sets, there seems to be another possibility of a non-linear wave coupling between a 2-day wave and the diurnal tide. Lieberman et al. (2017) use the global NOGAPS (Navy Operational Global Atmospheric Prediction System) ALPHA (Advanced Level Physics High Altitude) model to investigate a non-linear interaction between the migrating diurnal tide and the westward propagating quasi 2-day wave. This interaction results in a westward traveling wave component (W4) of zonal wave number 4 with an apparent period of 16 h and an eastward propagating wave of zonal wave number 2 with a period of 2 days. Amplitudes of W4 are largest in the mid-latitude winter mesosphere and the ~~lower and upper boundary of the considered atmospheric shear layer.~~

~~Table **??** summarizes the monthly mean magnitude of the bulk shear vector. The layer between 64 and has the highest average amount of bulk shear. In the considered time period , the values for February 2015 and 2016 reach its peak with around (). These high wind shear conditions are likely to be the reason why the GW activity above was low (Fig. **??**). Since the wind shear has a high temporal variability, occasionally low shear values occur and allow waves to travel higher up. Within the layer much lower bulk shear is found mostly between 20 and , which makes additional parameters necessary to explain the sharp boundary in temperature amplitudes right below . The location of the stratopause with the accompanied local temperature maximum at around altitude could have a significant effect on the propagation of waves~~wind magnitudes in the MLT reach typically $10\,\mathrm{m\,s^{-1}}$ in the model data. However wind amplitudes from meteor radar measurements at Bear Lake (42 °N, 111.3 °W) exceeded those from the NOGAPS ALPHA model system. The maximal zonal wind amplitudes of the 18-hour wave component observed by WIRA at a comparable latitude reach about $40\,\mathrm{m\,s^{-1}}$ in the mid-mesosphere. But the lower altitude of the WIRA measurements impede an acceptable comparison to results in the paper of Lieberman et al. (2017) .

The fact, that the W4 wave shows inertia-gravity wave-like features (Lieberman et al., 2017) and has a period within our defined quasi 18-hour period band, it is likely that we observed such a described W4 wave in our spectral data analyses. For November 2014, February and March 2015 the monthly mean amplitude peaks in the water vapor wave spectrum is closer to 16 h than to 18 h, which could be a clue for a W4 wave. In contrast to satellite observations, the temporal resolution of the local profile measurements, which our instruments provide, are not outside the Nyquist limits of temporal resolution for the westward traveling 16-hour W4 wave. The information of long-term microwave radiometric observations of non-linear wave-wave couplings such as W4 could be very useful to validate numerical model results.

5 Conclusion

For the first time a dominant quasi 18-hour wave in mesospheric water vapor has been reported from ground-based measurements. A unique data set from the MIAWARA instrument with a temporal resolution of 3 hours has been examined for wave

signatures with periods between 6–30 hours. Two winter time periods were used to present monthly mean wave spectra of H_2O. For a considerable number of months prominent wave signatures in the quasi 18-hour (15–21 hours) period band have been identified. The packet-like occurrence in time and growing amplitudes with decreasing pressure are ~~in agreement with~~ a inertia-gravity ~~wave characteristics~~wave-like feature.

In the first part of Sect. 4.3 we straightened out that our ground-based observations are robust and that the retrievals are not contaminated by any considerable artifacts. Whether the observed wave is a direct image of a low frequency ~~gravity~~ inertia-gravity wave is not definitely clear~~. A clear physical connection between the temporal coherence of 18-hour water vapor and wind amplitudes has not been found. But individual 18-hour amplitude profiles of MIAWARA and SD-WACCM regularly reach high correlation coefficients of more than 0.6 or less frequently even more than 0.8~~, but gravity waves with comparable frequencies have been observed at mesospheric altitudes in the winter hemisphere. Another promising clarification approach is the mentioned non-linear coupling of the quasi 2-day wave to the migrating diurnal tide. A much more detailed analysis of the quasi 2-day wave behavior above Bern is necessary to understand the complex interactions and wave couplings we maybe identified in mesospheric zonal wind and water vapor profile time series. This is an encouraging future research project.

It has been shown that the WIRA instrument is capable to resolve sub-diurnal oscillations, although a larger continuous observation time for such studies would be desirable. The quality of the WIRA meridional wind component measurements have ~~still~~ a potential for improvement and could contribute to wave characteristic analyses also in regard of validations to models. ~~In this study only a few days of WIRA measurements could be used to compare with MIAWARA and SD-WACCM. The MIAWARA , SD-WACCM and WIRA zonal wind wave patterns in December 2015 have shown temporal correlation with mismatch in altitude. The January 2016 case study did neither exhibit an obvious temporal nor vertical correlation between observed MIAWARA and SD-WACCM wind 18-hour wave signatures. By now we do not have a comprehensive understanding about the links between the observed quasi 18-hour wave in and wind, although water vapor should mostly be dynamically controlled in the mesosphere and sub-diurnal time range. Photochemistry and vertical transport have small impact on mesospheric water vapor leading to a mean lifetime on the order of weeks (Brasseur and Solomon, 2006) . We conclude that more sophisticated numerical model studies are needed, which go beyond the scope of this paper and our possibilities, to explain the found circumstance.~~

~~What has to be considered by comparing the appearance of wind and water vapor wave amplitudes is that the latter may only be observed where the vertical or horizontal gradient in the volume mixing ratio is high. This might lead to high differences and low qualitative correlations in time and space. It should be added that vertical and horizontal advection affect the variability. Further, as mentioned before, parameterized gravity wave effects in models are generally considered poorly constrained by observations (Fritts and Alexander, 2003) .~~

~~With single instrument observations of all necessary variables, such in Li et al. (2007) with a sodium-lidar, the identification of inertia-gravity wave characteristics is less interdependent. The disadvantage of single instrument observations is the possibility of measurement artifact spreading over all measured parameters. Independent observations of atmospheric wave patterns by different instruments can reduce misinterpretations.~~

~~Although the elliptical fit in our hodograph perturbation data is not perfect with the SD-WACCM model data, we show that meaningful inertia-gravity wave parameters can be identified: Intrinsic periods of about 14 hours, south-westward to westward propagation direction with downward phase progression, horizontal wavelengths of and and vertical wavelengths of less than . These results can foster future studies such as model validations to high quality observations from ground by for example radar, lidar or microwave instruments.~~

Author contributions. ML was responsible for the ground-based water vapor measurements, performed the data analysis and prepared the manuscript. KH designed the filter algorithm and contributed to the interpretation of the results. RR is in charge of WIRA, the ground based wind radiometer, and provided wind retrieval data. NK is the lead of the project group. All authors read and approved the current manuscript version and declare that they have no conflict of interest.

Acknowledgements. This work is supported by Swiss National Science Foundation Grant 200020-160048 and MeteoSwiss in the frame of the GAW project "Fundamental GAW parameters measured by microwave radiometry". Rolf Rüfenacht is supported by Post-doc Grant P2BEP2-165383. We acknowledge NASA for access to Aura MLS data and the NCAR CESM working group for providing the SD-WACCM model code.

References

Baumgarten, G., Fiedler, J., Hildebrand, J., and Lübken, F.-J.: Inertia gravity wave in the stratosphere and mesosphere observed by Doppler wind and temperature lidar, Geophys. Res. Lett., 42, 10,929–10,936, doi:10.1002/2015GL066991, 2015GL066991, 2015.

Belova, A., Kirkwood, S., Murtagh, D., Mitchell, N., Singer, W., and Hocking, W.: Five-day planetary waves in the middle atmosphere from Odin satellite data and ground-based instruments in Northern Hemisphere summer 2003, 2004, 2005 and 2007, Ann. Geophys., 26, 3557–3570, doi:10.5194/angeo-26-3557-2008, 2008.

Brasseur, G. and Solomon, S.: Aeronomy of the Middle Atmosphere: Chemistry and Physics of the Stratosphere and Mesosphere, vol. 32, Springer, 2006.

Charney, J. G. and Drazin, P. G.: Propagation of planetary-scale disturbances from the lower into the upper atmosphere, J. Geophys. Res., 66, 83–109, doi:10.1029/JZ066i001p00083, 1961.

Collins, W. D., Bitz, C. M., Blackmon, M. L., Bonan, G. B., Bretherton, C. S., Carton, J. A., Chang, P., Doney, S. C., Hack, J. J., Henderson, T. B., Kiehl, J. T., Large, W. G., McKenna, D. S., Santer, B. D., and Smith, R. D.: The Community Climate System Model Version 3 (CCSM3), J. Climate, 19, 2122–2143, doi:10.1175/JCLI3761.1, 2006.

Deuber, B., Kämpfer, N., and Feist, D. G.: A new 22-GHz Radiometer for Middle Atmospheric Water Vapour Profile Measurements, IEEE Trans. Geosci. Remote Sens., 42, 974–984, doi:10.1109/TGRS.2004.825581, 2004.

Deuber, B., Haefele, A., Feist, D. G., Martin, L., Kämpfer, N., Nedoluha, G. E., Yushkov, V., Khaykin, S., Kivi, R., and Vomel, H.: Middle Atmospheric Water Vapour Radiometer - MIAWARA: Validation and first results of the LAUTLOS / WAVVAP campaign, J. Geophys. Res., 110, D13 306, doi:10.1029/2004JD005543, 2005.

Emmons, L. K., Walters, S., Hess, P. G., Lamarque, J.-F., Pfister, G. G., Fillmore, D., Granier, C., Guenther, A., Kinnison, D., Laepple, T., Orlando, J., Tie, X., Tyndall, G., Wiedinmyer, C., Baughcum, S. L., and Kloster, S.: Description and evaluation of the Model for Ozone and Related chemical Tracers, version 4 (MOZART-4), Geosci. model dev., 3, 43–67, doi:10.5194/gmd-3-43-2010, 2010.

Eriksson, P., Jiménez, C., and Buehler, S. A.: Qpack, a general tool for instrument simulation and retrieval work, J. Quant. Spectrosc. Radiat. Transfer, 91, 47 – 64, doi:10.1016/j.jqsrt.2004.05.050, 2005.

Eriksson, P., Buehler, S., Davis, C., Emde, C., and Lemke, O.: ARTS, the atmospheric radiative transfer simulator, version 2, J. Quant. Spectrosc. Radiat. Transfer, 112, 1551 – 1558, doi:10.1016/j.jqsrt.2011.03.001, 2011.

Ern, M., Preusse, P., Alexander, M. J., and Warner, C. D.: Absolute values of gravity wave momentum flux derived from satellite data, J. Geophys. Res. Atmos., 109, doi:10.1029/2004JD004752, d20103, 2004.

Forbes, J. M.: Vertical coupling by the semidiurnal tide in Earth's atmosphere, Annual reviews, 2009.

Forbes, J. M., Hagan, M. E., Miyahara, S., Vial, F., Manson, A. H., Meek, C. E., and Portnyagin, Y. I.: Quasi 16-day oscillation in the mesosphere and lower thermosphere, J. Geophys. Res. Atmos., 100, 9149–9163, doi:10.1029/94JD02157, 1995.

Fritts, D. C. and Alexander, M. J.: Gravity wave dynamics and effects in the middle atmosphere, Rev. Geophys., 41, doi:10.1029/2001RG000106, 1003, 2003.

Fritts, D. C., Bizon, C., Werne, J. A., and Meyer, C. K.: Layering accompanying turbulence generation due to shear instability and gravity-wave breaking, J. Geophys. Res. Atmos., 108, doi:10.1029/2002JD002406, 8452, 2003.

Hagan, M. E. and Forbes, J. M.: Migrating and nonmigrating diurnal tides in the middle and upper atmosphere excited by tropospheric latent heat release, J. Geophys. Res. Atmos., 107, ACL 6–1–ACL 6–15, doi:10.1029/2001JD001236, 4754, 2002.

Han, Y. and Westwater, E. R.: Analysis and improvement of tipping calibration for ground-based microwave radiometers, IEEE Transactions on Geoscience and Remote Sensing, 38, 1260–1276, doi:10.1109/36.843018, 2000.

Hardiman, S. C., Butchart, N., Charlton-Perez, A. J., Shaw, T. A., Akiyoshi, H., Baumgaertner, A., Bekki, S., Braesicke, P., Chipperfield, M., Dameris, M., Garcia, R. R., Michou, M., Pawson, S., Rozanov, E., and Shibata, K.: Improved predictability of the troposphere using stratospheric final warmings, J. Geophys. Res. Atmos., 116, doi:10.1029/2011JD015914, d18113, 2011.

Harris, F. J.: On the use of windows for harmonic analysis with the discrete Fourier transform, Proc. IEEE, 66, 51–83, doi:10.1109/PROC.1978.10837, 1978.

Hines, C. O. and Reddy, C. A.: On the propagation of atmospheric gravity waves through regions of wind shear, J. Geophys. Res., 72, 1015–1034, doi:10.1029/JZ072i003p01015, 1967.

Hocke, K., Lainer, M., Moreira, L., Hagen, J., Fernandez Vidal, S., and Schranz, F.: Atmospheric inertia-gravity waves retrieved from level-2 data of the satellite microwave limb sounder Aura/MLS, Ann. Geophys., 34, 781–788, doi:10.5194/angeo-34-781-2016, 2016.

Jacobi, C., Schminder, R., and Kürschner, D.: Planetary wave activity obtained from long-period (2–18 days) variations of mesopause region winds over Central Europe (52 °N, 15 °E), J. Atmos. Sol.-Terr. Phy., 60, 81–93, doi:10.1016/S1364-6826(97)00117-X, 1998.

Kämpfer, N., Nedoluha, G., Haefele, A., and De Wachter, E.: Microwave Radiometry, vol. 10 of *ISSI Scientific Report Series*, Springer New York, doi:10.1007/978-1-4614-3909-7, 2012.

Kunz, A., Pan, L. L., Konopka, P., Kinnison, D. E., and Tilmes, S.: Chemical and dynamical discontinuity at the extratropical tropopause based on START08 and WACCM analyses, J. Geophys. Res. Atmos., 116, doi:10.1029/2011JD016686, d24302, 2011.

Labitzke, K., Austin, J., Butchart, N., Knight, J., Takahashi, M., Nakamoto, M., Nagashima, T., Haigh, J., and Williams, V.: The global signal of the 11-year solar cycle in the stratosphere: observations and models, J. Atmos. Sol.-Terr. Phy., 64, 203 – 210, doi:http://dx.doi.org/10.1016/S1364-6826(01)00084-0, sTEP-Results, Applications and Modelling Phase (S-RAMP), 2002.

Lainer, M., Kämpfer, N., Tschanz, B., Nedoluha, G. E., Ka, S., and Oh, J. J.: Trajectory mapping of middle atmospheric water vapor by a mini network of NDACC instruments, Atmos. Chem. Phys., 15, 9711–9730, doi:10.5194/acp-15-9711-2015, 2015.

Lainer, M., Hocke, K., and Kämpfer, N.: Variability of mesospheric water vapor above Bern in relation to the 27-day solar rotation cycle, J. Atmos. Sol.-Terr. Phy., 143–144, 71–87, doi:http://dx.doi.org/10.1016/j.jastp.2016.03.008, 2016.

Lamarque, J.-F., Emmons, L. K., Hess, P. G., Kinnison, D. E., Tilmes, S., Vitt, F., Heald, C. L., Holland, E. A., Lauritzen, P. H., Neu, J., Orlando, J. J., Rasch, P. J., and Tyndall, G. K.: CAM-chem: description and evaluation of interactive atmospheric chemistry in the Community Earth System Model, Geosci. model dev., 5, 369–411, doi:10.5194/gmd-5-369-2012, 2012.

Li, T., She, C.-Y., Liu, H.-L., Leblanc, T., and McDermid, I. S.: Sodium lidar–observed strong inertia-gravity wave activities in the mesopause region over Fort Collins, Colorado (41°N, 105°W), J. Geophys. Res. Atmos., 112, doi:10.1029/2007JD008681, d22104, 2007.

Lieberman, R. S., Riggin, D. M., Nguyen, V., Palo, S. E., Siskind, D. E., Mitchell, N. J., Stober, G., Wilhelm, S., and Livesey, N. J.: Global observations of 2 day wave coupling to the diurnal tide in a high-altitude forecast-assimilation system, Journal of Geophysical Research: Atmospheres, 122, 4135–4149, doi:10.1002/2016JD025144, 2016JD025144, 2017.

Limpasuvan, V., Richter, J. H., Orsolini, Y. J., Stordal, F., and Kvissel, O.-K.: The roles of planetary and gravity waves during a major stratospheric sudden warming as characterized in {WACCM}, J. Atmos. Sol.-Terr. Phy., 78–79, 84–98, doi:http://dx.doi.org/10.1016/j.jastp.2011.03.004, structure and Dynamics of Mesosphere and Lower Thermosphere, 2012.

Lin, S.-J. and Rood, R. B.: An explicit flux-form semi-lagrangian shallow-water model on the sphere, Quart. J. Roy. Meteor. Soc., 123, 2477–2498, doi:10.1002/qj.49712354416, 1997.

Lindzen, R. S.: Turbulence and stress owing to gravity wave and tidal breakdown, J. Geophys. Res. Oceans, 86, 9707–9714, doi:10.1029/JC086iC10p09707, 1981.

Liu, H.-L. and Meriwether, J. W.: Analysis of a temperature inversion event in the lower mesosphere, J. Geophys. Res. Atmos., 109, doi:10.1029/2002JD003026, d02S07, 2004.

Liu, J., Tarasick, D. W., Fioletov, V. E., McLinden, C., Zhao, T., Gong, S., Sioris, C., Jin, J. J., Liu, G., and Moeini, O.: A global ozone climatology from ozone soundings via trajectory mapping: a stratospheric perspective, Atmos. Chem. Phys., 13, 11 441–11 464, doi:10.5194/acp-13-11441-2013, 2013.

Livesey, N. J., Read, W. G., Wagner, P. A., Froidevaux, L., Lambert, A., Manney, G. L., Millán Valle, L. F., Pumphrey, H. C., Santee, M. L., Schwartz, M. J., Wang, S., Fuller, R. A., Jarnot, R. F., Knosp, B. W., and Martinez, E.: Version 4.2x Level 2 data quality and description document, Tech. rep., Jet Propulsion Laboratory, California Institute of Technology, 2015.

Maekawa, Y., Fukao, S., Sato, T., Kato, S., and Woodman, R. F.: Internal Inertia–Gravity Waves in the Tropical Lower Stratosphere Observed by the Arecibo Radar, J. Atmos. Sci., 41, 2359–2367, doi:10.1175/1520-0469(1984)041<2359:IIWITT>2.0.CO;2, 1984.

Marsh, D. R., Mills, M. J., Kinnison, D. E., Lamarque, J.-F., Calvo, N., and Polvani, L. M.: Climate Change from 1850 to 2005 Simulated in CESM1(WACCM), J. Climate, 26, 7372–7391, doi:10.1175/JCLI-D-12-00558.1, 2013.

McDonald, A. J., Hibbins, R. E., and Jarvis, M. J.: Properties of the quasi 16 day wave derived from EOS MLS observations, J. Geophys. Res. Atmos., 116, D06 112, doi:10.1029/2010JD014719, 2011.

McFarlane, N. A.: The Effect of Orographically Excited Gravity Wave Drag on the General Circulation of the Lower Stratosphere and Troposphere, J. Atmos. Sci., 44, 1775–1800, doi:10.1175/1520-0469(1987)044<1775:TEOOEG>2.0.CO;2, 1987.

Nappo, C. J.: An introduction to atmospheric gravity waves, Academic Press, 2002.

Nicolls, M. J., Varney, R. H., Vadas, S. L., Stamus, P. A., Heinselman, C. J., Cosgrove, R. B., and Kelley, M. C.: Influence of an inertia-gravity wave on mesospheric dynamics: A case study with the Poker Flat Incoherent Scatter Radar, J. Geophys. Res. Atmos., 115, doi:10.1029/2010JD014042, 2010.

Oppenheim, A. V., Schafer, R. W., Buck, J. R., et al.: Discrete-time signal processing, vol. 2, Prentice-hall Englewood Cliffs, 1989.

Orr, A., Bechtold, P., Scinocca, J., Ern, M., and Janiskova, M.: Improved Middle Atmosphere Climate and Forecasts in the ECMWF Model through a Nonorographic Gravity Wave Drag Parameterization, J. Climate, 23, 5905–5926, doi:10.1175/2010JCLI3490.1, 2010.

Plougonven, R. and Teitelbaum, H.: Comparison of a large-scale inertia-gravity wave as seen in the ECMWF analyses and from radiosondes, Geophys. Res. Lett., 30, doi:10.1029/2003GL017716, 1954, 2003.

Plougonven, R. and Zhang, F.: Internal gravity waves from atmospheric jets and fronts, Rev. Geophys., 52, 33–76, doi:10.1002/2012RG000419, 2014.

Riggin, D. M., Liu, H.-L., Lieberman, R. S., Roble, R. G., III, J. M. R., Mertens, C. J., Mlynczak, M. G., Pancheva, D., Franke, S. J., Murayama, Y., Manson, A. H., Meek, C. E., and Vincent, R. A.: Observations of the 5-day wave in the mesosphere and lower thermosphere, J. Atmos. Sol.-Terr. Phy., 68, 323 – 339, doi:10.1016/j.jastp.2005.05.010, 2006.

Rodgers, C. D.: Inverse methods for atmospheric sounding: theory and practice, vol. 2, World Scientific Publishing Co Pte. Ltd., 2000.

Rodgers, C. D. and Prata, A. J.: Evidence for a traveling two-day wave in the middle atmosphere, J. Geophys. Res. Oceans, 86, 9661–9664, doi:10.1029/JC086iC10p09661, 1981.

Rosenlof, K. H. and Thomas, R. J.: Five-day mesospheric waves observed in Solar Mesosphere Explorer ozone, J. Geophys. Res. Atmos., 95, 895–899, doi:10.1029/JD095iD01p00895, 1990.

Rüfenacht, R., Kämpfer, N., and Murk, A.: First middle-atmospheric zonal wind profile measurements with a new ground-based microwave Doppler-spectro-radiometer, Atmos. Meas. Tech., 5, 2647–2659, doi:10.5194/amt-5-2647-2012, 2012.

Rüfenacht, R., Murk, A., Kämpfer, N., Eriksson, P., and Buehler, S. A.: Middle-atmospheric zonal and meridional wind profiles from polar, tropical and midlatitudes with the ground-based microwave Doppler wind radiometer WIRA, Atmos. Meas. Tech., 7, 4491–4505, doi:10.5194/amt-7-4491-2014, 2014.

Rüfenacht, R., Hocke, K., and Kämpfer, N.: First continuous ground-based observations of long period oscillations in the vertically resolved wind field of the stratosphere and mesosphere, Atmospheric Chemistry and Physics, 16, 4915–4925, doi:10.5194/acp-16-4915-2016, 2016.

Ruzmaikin, A., Santee, M. L., Schwartz, M. J., Froidevaux, L., and Pickett, H. M.: The 27-day variations in stratospheric ozone and temperature: New MLS data, Geophys. Res. Lett., 34, doi:10.1029/2006GL028419, l02819, 2007.

Salby, M. L.: The 2-day wave in the middle atmosphere: Observations and theory, J. Geophys. Res. Oceans, 86, 9654–9660, doi:10.1029/JC086iC10p09654, 1981a.

Salby, M. L.: Rossby Normal Modes in Nonuniform Background Configurations. Part I: Simple Fields, J. Atmos. Sci., 38, 1803–1826, doi:10.1175/1520-0469(1981)038<1803:RNMINB>2.0.CO;2, 1981b.

Sawyer, J. S.: Quasi-periodic wind variations with height in the lower stratosphere, Quart. J. Roy. Meteor. Soc., 87, 24–33, doi:10.1002/qj.49708737104, 1961.

Scheiben, D., Schanz, A., Tschanz, B., and Kämpfer, N.: Diurnal variations in middle-atmospheric water vapor by ground-based microwave radiometry, Atmospheric Chemistry and Physics, 13, 6877–6886, doi:10.5194/acp-13-6877-2013, 2013.

Scheiben, D., Tschanz, B., Hocke, K., Kämpfer, N., Ka, S., and Oh, J. J.: The quasi 16-day wave in mesospheric water vapor during boreal winter 2011/2012, Atmos. Chem. Phys., 14, 6511–6522, doi:10.5194/acp-14-6511-2014, 2014.

Schmidlin, F. J.: Rocket techniques used to measure the neutral atmosphere, Middle Atmosphere Program, Handbook for MAP, 19, R. A. Goldberg, 1–33, SCOSTEP Secretariat, Univ. of Ill., Urbana, 1986.

Shapiro, A. V., Rozanov, E., Shapiro, A. I., Wang, S., Egorova, T., Schmutz, W., and Peter, T.: Signature of the 27-day solar rotation cycle in mesospheric OH and H₂O observed by the Aura Microwave Limb Sounder, Atmos. Chem. Phys., 12, 3181–3188, doi:10.5194/acp-12-3181-2012, 2012.

Shapiro, M. A. and Keyser, D. A.: Fronts, jet streams, and the tropopause, US Department of Commerce, National Oceanic and Atmospheric Administration, Environmental Research Laboratories, Wave Propagation Laboratory, 1990.

Studer, S., Hocke, K., and Kämpfer, N.: Intraseasonal oscillations of stratospheric ozone above Switzerland, J. Atmos. Sol.-Terr. Phy., 74, 189 – 198, doi:10.1016/j.jastp.2011.10.020, 2012.

Tschanz, B. and Kämpfer, N.: Signatures of the 2-day wave and sudden stratospheric warmings in Arctic water vapour observed by ground-based microwave radiometry, Atmos. Chem. Phys., 15, 5099–5108, doi:10.5194/acp-15-5099-2015, 2015.

Tsuda, T., Kato, S., Yokoi, T., Inoue, T., Yamamoto, M., VanZandt, T. E., Fukao, S., and Sato, T.: Gravity waves in the mesosphere observed with the middle and upper atmosphere radar, Radio Sci., 25, 1005–1018, doi:10.1029/RS025i005p01005, 1990.

Wu, D. L., Hays, P. B., and Skinner, W. R.: Observations of the 5-day wave in the mesosphere and lower thermosphere, Geophys. Res. Lett., 21, 2733–2736, doi:10.1029/94GL02660, 1994.

Yue, J., Liu, H.-L., and Chang, L. C.: Numerical investigation of the quasi 2 day wave in the mesosphere and lower thermosphere, J. Geophys. Res. Atmos., 117, D05 111, doi:10.1029/2011JD016574, 2012.

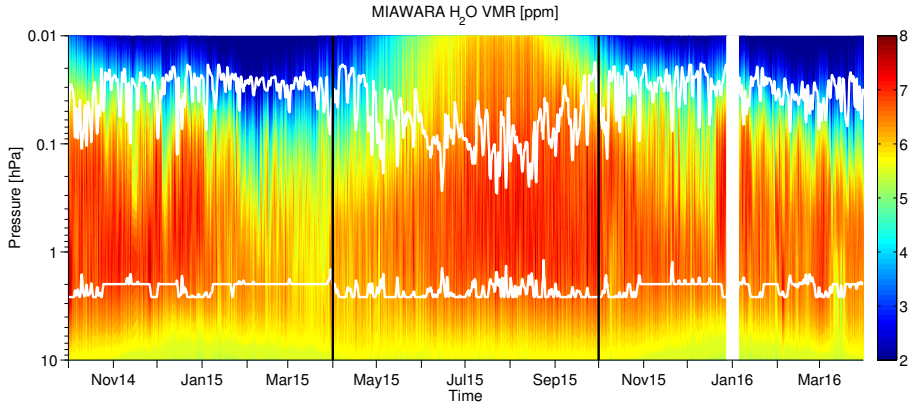

Figure 1. The water vapor volume mixing ratio [ppm] time series measured by MIAWARA between October 2014 and March 2016. The horizontal white lines indicate at which pressure levels the measurement response drops below 80 %. During the more humid and warm season between April and September 2015 the data will not be used. This is marked by the vertical black lines. A measurement gap occurred between 2015-12-28 and 2016-01-04 as shown by the white bar.

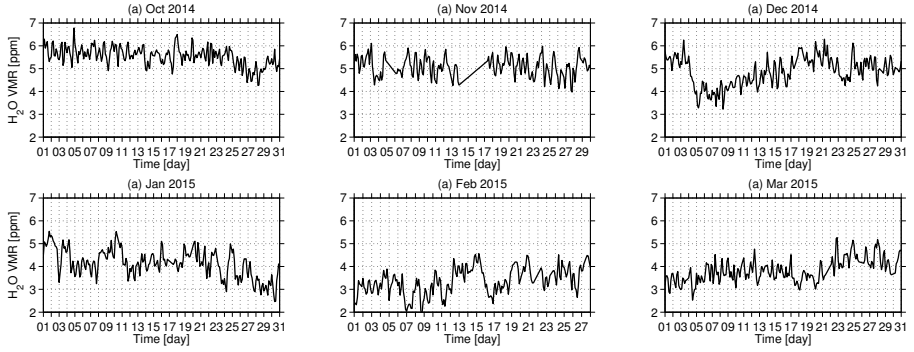

Figure 2. Monthly time series of MIAWARA H_2O averaged between 0.02 and 0.1 hPa for winter 2014/2015.

Zhang, F., Wang, S., and Plougonven, R.: Uncertainties in using the hodograph method to retrieve gravity wave characteristics from individual soundings, Geophys. Res. Lett., 31, doi:10.1029/2004GL019841, l11110, 2004.

~~Monthly mean magnitude of bulk shear vector ms^{-1} calculated from SD-WACCM model output within four different middle atmospheric layers of depth. The time period from October 2014 to March 2015 (upper panel) and October 2015 to March 2016 (lower panel) is covered.~~

~~Oct 2014 Nov 2014 Dec 2014 Jan 2015 Feb 2015 Mar 201533.2 59.7 43.0 43.9 73.7 55.724.5 28.5 34.7 28.9 26.4 26.713.0 30.8 28.6 36.5 29.8 18.016.8 40.5 31.2 27.4 45.9 28.7~~

~~Oct 2015 Nov 2015 Dec 2015 Jan 2016 Feb 2016 Mar 201638.6 52.1 59.7 59.2 65.1 36.520.4 28.9 31.2 41.3 29.6 31.014.1 21.6 23.5 23.7 15.3 16.317.2 35.6 43.8 20.2 36.0 21.7~~

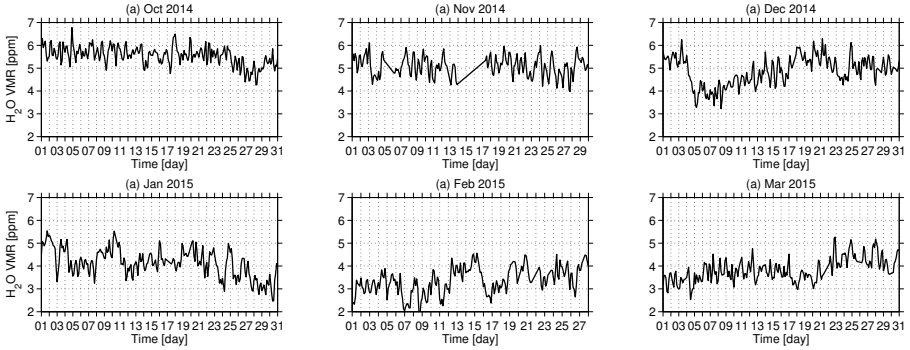

Figure 3. Same as Fig. 2, but for winter 2015/2016.

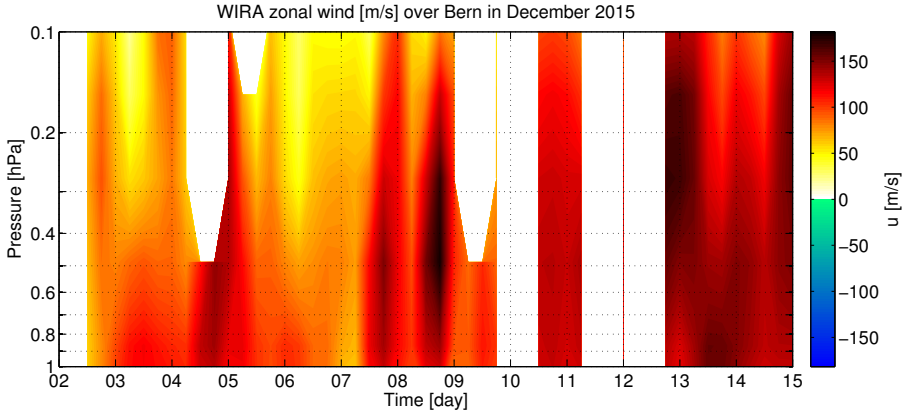

Figure 4. The zonal wind vector component time series measured by WIRA between 2015-12-05 and 2015-12-09 in the pressure range 0.1–1 hPa.

~~The SD-WACCM water vapor monthly mean wave spectrum with periods between 6 and 30 hours. Shown is the result of the amplitudes ppmfor the months January (a) and February (b) 2016. The border of the quasi 18-hour period band (15–21 hours) is indicated by the vertical black line pair.~~

~~Same as Fig. **??**, but here the time period from October 2015 to March 2016 is shown.~~

~~Filled area plot of Pearson product-moment correlation coefficient between MIAWARA and SD-WACCM quasi 18-hour () wave amplitude profile time series (in blue). In (a) the time period from 2014-10-01 to 2015-03-31 and in (b) from 2015-10-01 to 2016-03-31 is considered. Here only significant correlation coefficients (confidence interval) are plotted.~~

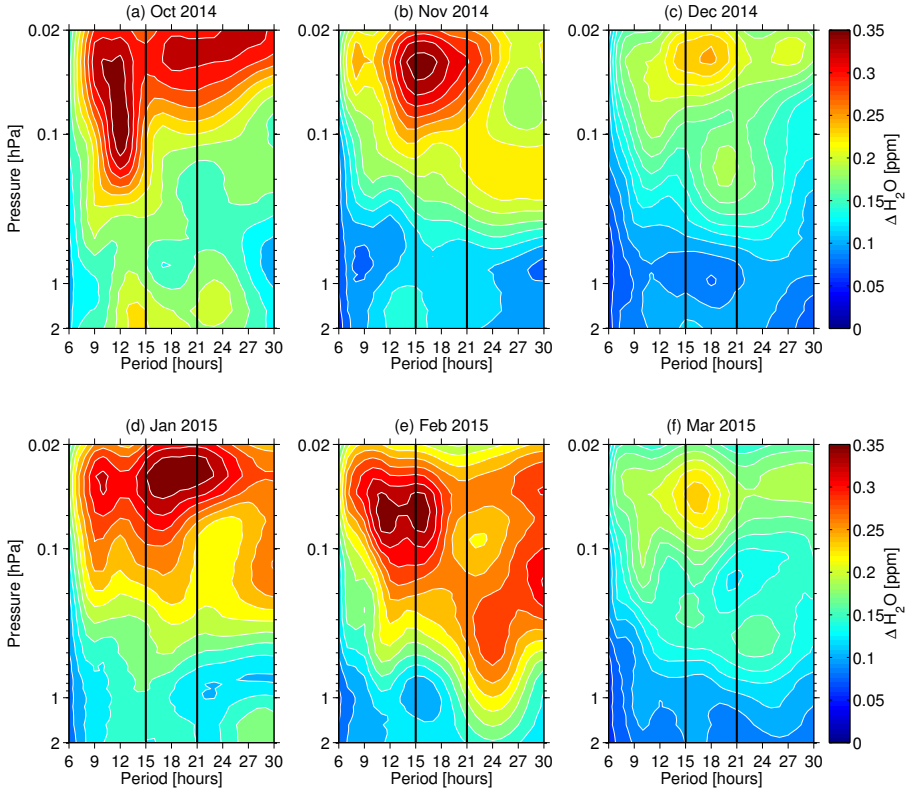

Figure 5. The MIAWARA water vapor monthly mean wave spectrum with periods between 6 and 30 hours. Shown is the result of the H_2O amplitudes [ppm] for the months October 2014 to March 2015 (a–f). The border of the quasi 18-hour period band (15–21 hours) is indicated by the vertical black line pair.

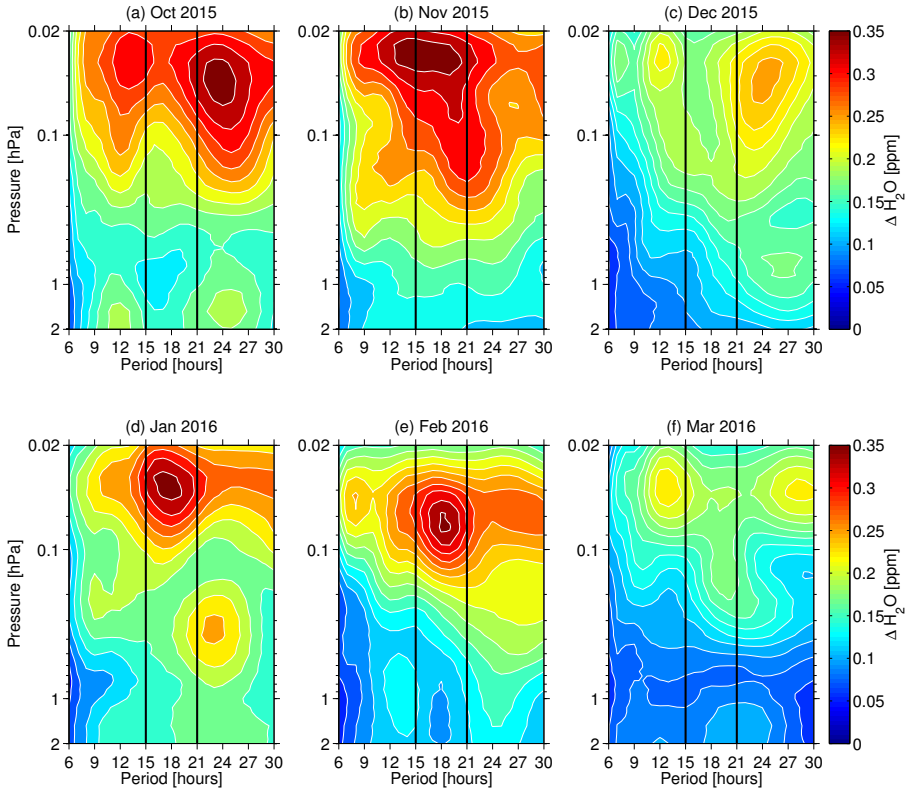

Figure 6. Same as Fig. 5, but ~~here we focus on~~ for the months October 2015 to March 2016 (a–f).

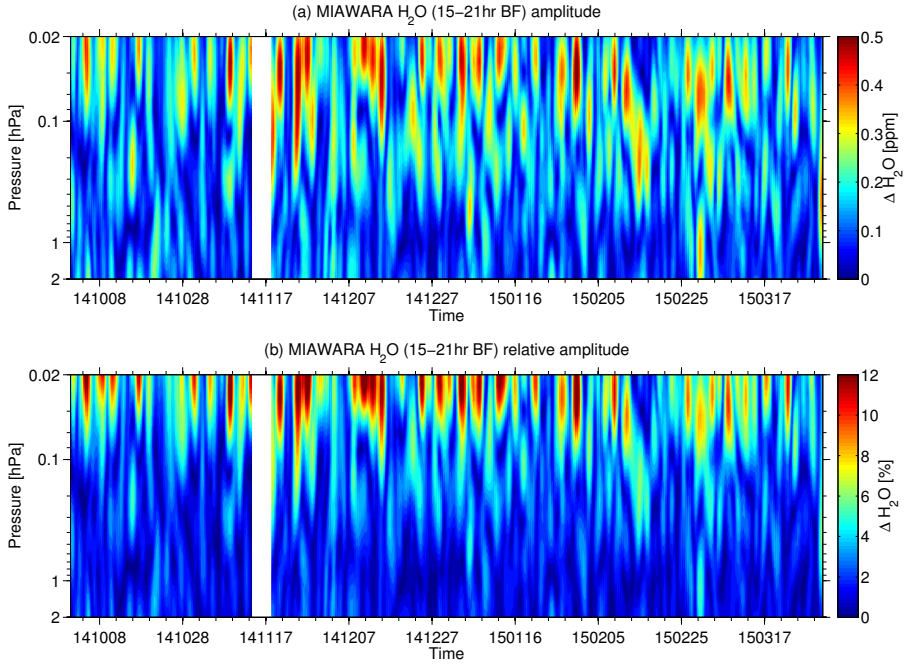

Figure 7. Temporal evolution of wave amplitudes derived from band-pass hamming-window filtered MIAWARA H_2O VMR time series with cut-off periods at 15 and 21 hours. Shown is the time period from October 2014 to March 2015.

~~Temporal evolution of wave amplitudes derived from band-pass hamming-window filtered SD-WACCM VMR time series with cut-off periods at 15 and 21 hours. Shown is the location of Bern and the time period from October 2014 to March 2015.~~

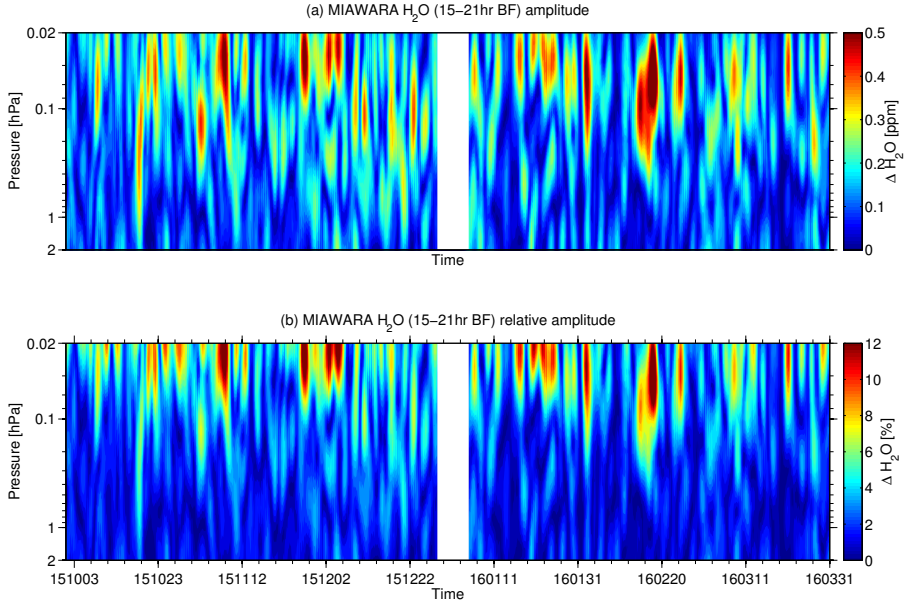

Figure 8. Same as Fig. 7, but here the time period from October 2015 to March 2016 is shown. The measurement gap between 2015-12-28 and 2016-01-04 is indicated by the white bar.

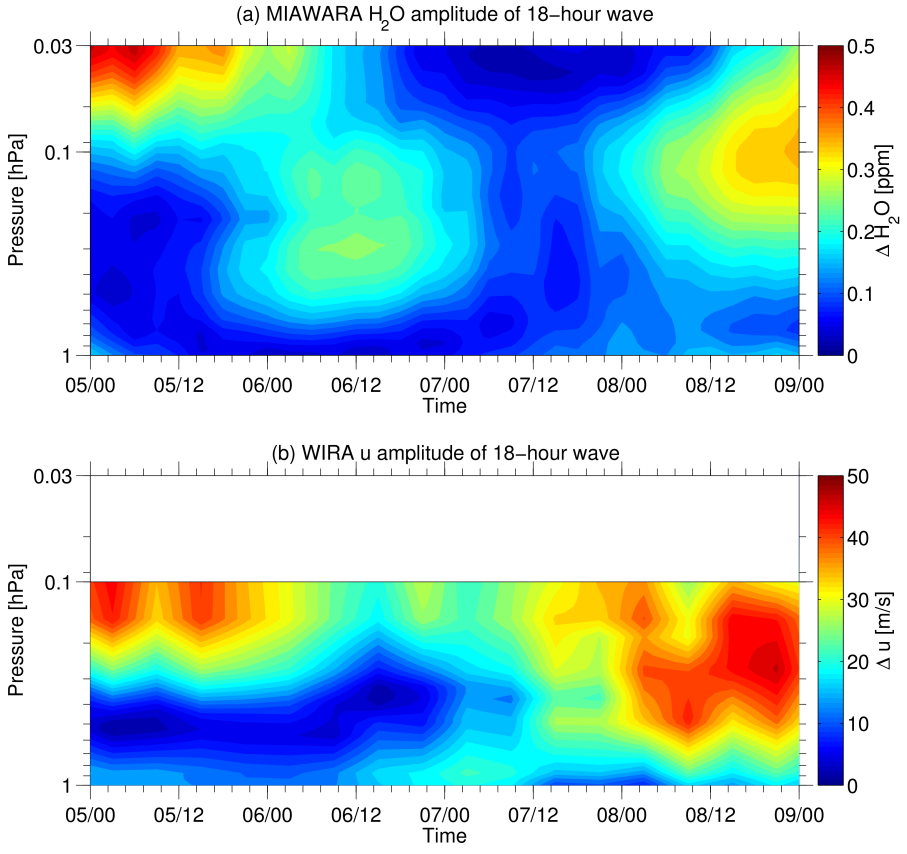

Figure 9. 18-hour band-pass filtered absolute wave amplitudes in the pressure range 0.03–1 hPa between 2015-12-05 and 2015-12-09. Upper panel (a) shows water vapor amplitudes as observed by MIAWARA, middle panel (b) shows zonal wind amplitudes as observed by WIRA~~and the bottom panel shows the zonal wind amplitudes from SD-WACCM model simulations~~.

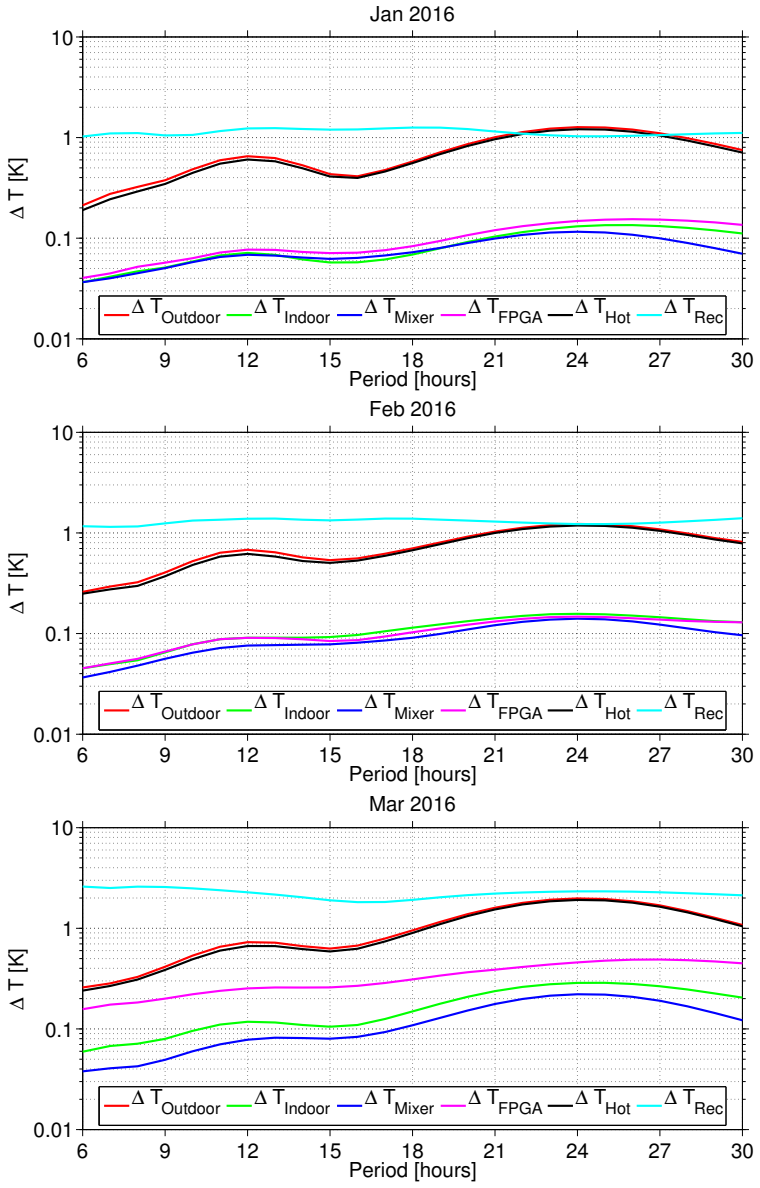

Figure 10. ~~18-hour band-pass absolute~~ Monthly mean spectral wave ~~amplitudes in~~ analysis for 6 different temperature parameters related to the ~~pressure range between 2016-01-16 and 2016-01-26. Upper panel (a) shows~~ MIAWARA water vapor ~~amplitudes as observed by MIAWARA~~radiometer: outdoor, ~~middle panel (b) shows zonal~~ indoor, mixer, FPGA, Hot-Load and ~~the bottom panel (c) meridional wind amplitudes~~ receiver temperature. Spectral analysis goes from ~~SD-WACCM model simulations~~6 to 30 hours with a resolution of 1 hour. The ~~vertical black lines mark the dates~~ results are shown for January, February and ~~pressure ranges of the exemplary hodograph analyzes (Fig. ??).~~March 2016.

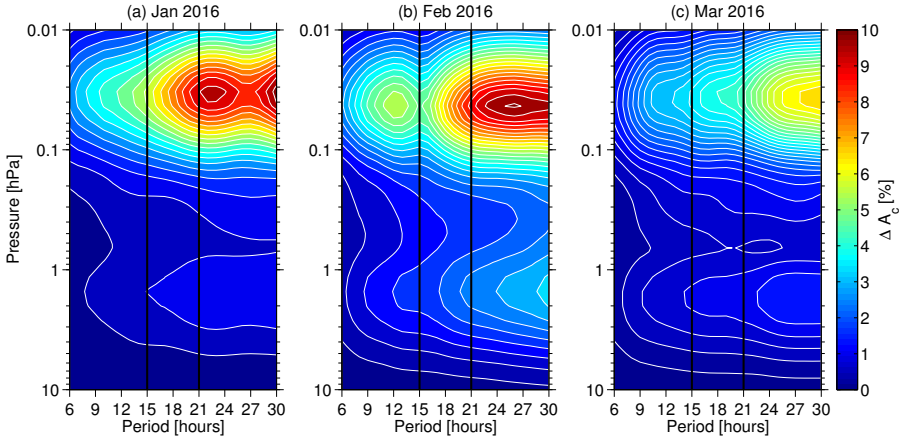

Figure 11. ~~Upper panels (a,b) show the hodograph~~ Monthly mean wave spectra of the ~~18-hour SD-WACCM zonal and meridional wind perturbations. An elliptical fit (red) is applied to the data points. Wave propagation direction k is indicated by the black arrow. Embedded~~ a priori contribution in the ~~hodograph figures,~~ MIAWARA water vapor retrievals for periods between 6 and 30 hours. Shown are ~~the vertical profiles~~ absolute wave amplitudes of the ~~background wind speed profiles projected onto the k -direction. The used color scheme separates different pressure levels~~a priori contribution in [%] for January (a), ~~from blue to red means increasing altitude~~ February (~~decreasing pressure~~b) ~~. Lower panels~~ and March (c,~~d~~) ~~show accordant to the overlying hodographs profiles of the vertical, eastward and northward 18-hour wind perturbations.~~ 2016.

~~Vertical high-pass filtered Aura MLS temperature profiles from 2014-10-01 to 2015-03-31 (a) and from 2015-10-01 to 2016-03-31 (b). High frequencies in the temperature profiles are passed through, i.e. with vertical wavelengths λ_z . The plot shows the filtered temperature oscillations ΔT_{HF} in the altitude range .~~